STEVENS INSTITUTE
OF TECHNOLOGY

CASTLE POINT STATION
HOBOKEN, NEW JERSEY 07030

NASA CR- 132346

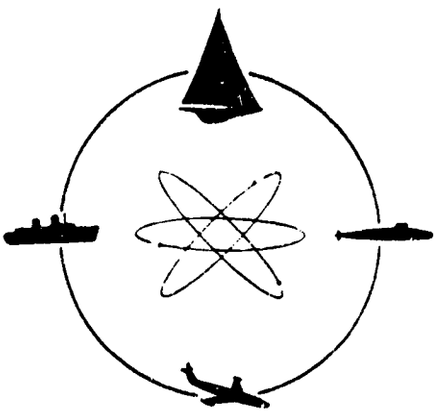

DAVIDSON LABORATORY

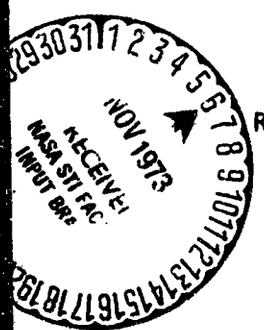

Report SIT-DL-72-1602

July 1973

A SYSTEMATIC EXPERIMENTAL INVESTIGATION OF SIGNIFICANT PARAMETERS AFFECTING MODEL TIRE HYDROPLANING

by

Gilbert A. Wray

Prepared for

NATIONAL AERONAUTICS AND SPACE ADMINISTRATION

NASA CR- 132346

September 1973

A SYSTEMATIC EXPERIMENTAL INVESTIGATION OF SIGNIFICANT PARAMETERS AFFECTING MODEL TIRE HYDROPLANING

By

Gilbert A. Wray

and

I. Robert Ehrlich

Prepared as Report SIT-DL-72-1602

under

Contract NAS 1-9349

by

DAVIDSON LABORATORY
Stevens Institute of Technology
Castle Point Station
Hoboken, N. J. 07030

(DL Projects 3628/480/464/465)

for

NATIONAL AERONAUTICS AND SPACE ADMINISTRATION

A SYSTEMATIC EXPERIMENTAL INVESTIGATION OF SIGNIFICANT PARAMETERS AFFECTING MODEL TIRE HYDROPLANING

by

Gilbert A. Wray

and

I. Robert Ehrlich

ABSTRACT

The results of a comprehensive parametric study of model and small pneumatic tires operating on a wet surface are presented. Hydroplaning inception (spin down) and rolling restoration (spin up) are discussed.

Conclusions indicate that hydroplaning inception occurs at a speed significantly higher than the rolling restoration speed. Hydroplaning speed increases considerably with tread depth, surface roughness and tire inflation pressure or footprint pressure, and only moderately with increased load. Water film thickness affects spin down speed only slightly. Spin down speed varies inversely as approximately the one-sixth power of film thickness.

Empirical equations relating tire inflation pressure, normal load, tire diameter and water film thickness have been generated for various tire tread and surface configurations.

Keywords

Tires

Tire Hydroplaning

Traction

Wet Runways

CONTENTS

A SYSTEMATIC EXPERIMENTAL INVESTIGATION OF SIGNIFICANT PARAMETERS AFFECTING MODEL TIRE HYDROPLANING

By Gilbert A. Wray and I. Robert Ehrlich
Stevens Institute of Technology

SUMMARY

A systematic study of the significant parameters affecting pneumatic tire hydroplaning when operating on wet surfaces was performed.

Scale model tires were constructed using an open celled polyurethane foam. The foam density was varied in order to match the load-deflection and footprint characteristics of a pneumatic tire. A "dimensionless analysis" study was performed to determine what the combination of significant tire parameters should be in order to facilitate correlation with full scale tires. A test program was then planned which would generate the required input data to the results of our "dimensionless analysis."

The model tires were tested on our "rolling road" facility. This apparatus permits us to operate a tire at various loads, on a moving belt surface while maintaining a water film of any desired thickness, within our operating range. The speed of the belt may be varied, and by varying the water flow rate through our nozzle, a film of water of specified thickness is placed on the belt at synchronous speed so that there is no relative velocity between the belt and the water film. By a process of iteration a speed is obtained whereby the wheel spontaneously spins down at the desired synchronous film thickness.

Tests were performed on an 8-inch diameter, smooth polyurethane tire operating on a smooth road surface. The normal load was varied from 5 lb to 70 lb and the water film thickness varied from 0.021 inch to 0.125 inch. Both spin down and spin up (rolling restoration) speeds were measured. The tire was then modified to have 4 and 8 ribs of 1/32, 2/32 and 3/32 inch depth, and the spin down speeds determined for all combinations of tread depth, number of ribs, load and water film thickness.

From the above tests it was determined that the tire "contact patch bearing pressure" has the largest single effect on spin down speed. Increasing "bearing pressure" caused the tire to "spin down" at a higher speed. Tire normal load

has a moderate effect insofar as it increases the footprint bearing pressure (on a polyurethane model tire).

The water film thickness has only a slight effect on spin down speed; the hydroplaning speed varying inversely as approximately the one-sixth power of film thickness.

Due to difficulty in varying the tire contact patch bearing pressure of a polyurethane tire and relating it to the load and inflation pressure of a pneumatic tire it was decided to test a small pneumatic tire.

An 8-inch diameter by 2.80 inch cross-section pneumatic tire was selected for testing. This type of tire was tested in both the bald condition, and with a standard depth rib-groove tread pattern, on both a smooth road surface and a rough road surface. The rough surface was formed from strips of #150 grit abrasive cloth. The various combinations of tire tread and road surface were tested for all combinations of tire inflation pressure from 5 psi to 30 psi, loads from 5 lb to 120 lb and water film thicknesses from 0.021 to 0.125. Empirical equations relating tire pressure, diameter, normal load and water film thickness to hydroplaning inception speed (spin down speed) were derived for each tire-road configuration.

The empirical equations were checked against some published experimental data. The correlation between prediced spin down speed from our equation and measured data on full size tires was found to be quite good.

INTRODUCTION

It has long been recognized that a pneumatic tire rolling over a wet surface may encounter a condition whereby the tire rides up on the water film, much like a water skier or surfboard, resulting in a complete loss of traction. This condition is created when the tire and/or road surface cannot drain the water away from the advancing tire contact patch sufficiently quick. The water forms a wedge or bow wave in front of the tire, which due to its dynamic dynamic pressure begins to support part of the wheel/tire load and reduces the contact patch footprint area in contact with the road. This condition is generally referred to as partial hydroplaning. When the tire load is

completely supported by the water film the tire has lost all contact with the road surface as is said to be hydroplaning. In this state the tire has lost all contact with the road surface and cannot generate any tractive force. If allowed to roll freely (i.e., front wheels) the wheel will spin down and rotate at a slower speed, or stop completely.

Previous studies have shown that the effects of various tire and road parameters should be investigated more thoroughly.

The Davidson Laboratory and others have conducted both experimental[1,2,3,4,5] and theoretical[6,7] studies in an attempt to isolate the effects of various tire/road parameters such as inflation pressure, normal load, water film thickness, tread depth and road surface roughness. This experimental program was conducted on the Davidson Laboratory Rolling Road Facility.[8]

This report describes the results obtained by utilizing polyurethane model tires similar to those reported on in reference 3. The operating range of load and water film thickness was extended and the effects of the number of ribs and rib depth were also investigated. A similar size pneumatic tire was tested for the complete range of load (5-120 lb), tire inflation pressure (5 to 30 psig) and water film thickness (.021 to .125 inch). In addition this pneumatic tire was tested in the bald and full tread condition on both a smooth road surface and a rough road surface.

Additional testing was performed to determine the relationship between hydroplaning inception speed (spin down) and rolling restoration speed (spin up) which were previously found to differ considerably.

The author wishes to acknowledge the considerable assistance given by Major James R. Allred during the test program and data analysis. Mr. Awni Boutros provided needed assistance in generating a computer program for data and error analysis. Also, Miss Nancy Crane provided editorial assistance in addition to typing the manuscript.

SYMBOLS

a	acceleration
A	dimensionless constant
b	tire tread depth
B	dimensionless constant
B. P.	tire bearing pressure
c_i	exponentials used in dimensional analysis
C	dimensionless constant
c_α	dimensionless constant
D	tire undeflected diameter
F	force
F_V	vertical lift force
F_H	horizontal drag force
g	acceleration of gravity
h	fluid film thickness
l	length
m	exponential used in dimensional analysis
MHR	mean hydraulic radius of channels between surface asperities
P	tire inflation pressure, pressure
q	exponential used in dimensional analysis
Q	water flow rate
r	tire undeflected radius
v	velocity
V	belt speed, ground speed, vehicle forward speed
V_{cr-d}	spin down or critical hydroplaning speed
V_{cr-u}	spin up speed
w	tire contact patch width
W	vertical load on tire
λ	model scaling factor
μ	fluid dynamic viscosity
π_i	dimensionless parameter groups (Buckingham's Theorem)
$\bar{\pi}_i$	parameter groups held constant
ρ	fluid density

ANALYSIS

In order to set up a systematic test program it is necessary to determine what the significant parameters are. In this program scale model tires are being utilized and hence it is more convenient to express the primary variables in terms of dimensionless parameters.

By designing the test program so as to vary only one of the dimensionless parameters at a time, while maintaining the others constant, a relationship between the variables may be obtained.

By expressing the relationships in terms of dimensionless parameters correlation with full scale data is facilitated. The individual input variables such as wheel diameter, tire pressure, etc., do not have to be scaled by various powers of the scale factor.

The following is a list of the independent variables considered to have a significant effect on the hydroplaning inception (spin down) speed of a pneumatic tire rolling freely on a wet surface. The dimensional units considered are the FLT system, i.e., force is in pounds. Time is in seconds, distance is in feet.

Symbol	Description	FLT Units
D	tire undeflected diameter	L
w	tire section width	L
h	fluid film thickness	L
W	vertical load on tire	F
P	tire inflation pressure	FL^{-2}
b	tire tread depth	L
MHR	road surface MHR	L
ρ	fluid density	FL^{-3}
μ	fluid viscosity	$FL^{-2}T$
g	acceleration of gravity	LT^{-2}
V	hydroplaning inception speed (spin down)	LT^{-1}

Using the techniques of dimensional analysis a relationship expressing the dependency of spin down speed (V_{cr-d}) on the above variables may be derived.[3]

If we let

$$V = f(D,w,h,W,P,b,MHR,\rho,\mu,g) \tag{1}$$

Then on rearranging terms and assigning exponents to each of the variables

$$1 = C_\alpha V^{c_1} D^{c_2} w^{c_3} h^{c_4} W^{c_5} P^{c_6} b^{c_7} MHR^{c_8} \rho^{c_9} \mu^{c_{10}} g^{c_{11}} \tag{2}$$

where C_α = constant

c_1 to c_{11} = unknown exponents

Equation (2) expressed in terms of the dimensions associated with each variable is:

$$0 = (LT^{-1})^{c_1} L^{c_2} L^{c_3} L^{c_4} F^{c_5} (FL^{-2})^{c_6} L^{c_7} L^{c_8} (FL^{-3})^{c_9} (FL^{-2}T)^{c_{10}} (LT^{-2})^{c_{11}} \tag{3}$$

Grouping each of the three types of units (F,L,T) together and equating them to zero yields the following three auxiliary equations.

$$F: \quad 0 = c_5 + c_6 + c_9 + c_{10} \tag{4}$$

$$L: \quad 0 = c_1 + c_2 + c_3 + c_4 - 2c_6 + c_7 + c_8 - 3c_9 - 2c_{10} + c_{11} \tag{5}$$

$$T: \quad 0 = -c_1 + c_{10} - 2c_{11} \tag{6}$$

Since we have eleven unknowns and only three equations available, arbitrary values must be assigned to 8 of the unknowns. The selection of unknowns to be assigned values and the value assigned is arbitrary provided the determinant of the coefficients of the remaining terms is not zero.

Selecting $c_5, c_4, c_6, c_8, c_7, c_2, c_9$ and c_{11} as our candidates to have values assigned to them we obtain for the determinant of the remaining coefficients

$$\begin{vmatrix} 0 & 0 & 1 \\ 1 & 1 & -2 \\ -1 & 0 & 1 \end{vmatrix} = 1 \qquad (7)$$

Since the determinant is non-zero our selection is valid and the values to be assigned are arbitrarily chosen to be zero for all terms except one of them which is assigned to the value of 1. The auxiliary equations are then solved and a π term obtained. By repeating this process until each of the 8 unknowns have been assigned the value 1 we obtain all our π terms. Note that if values other than zero and 1 had been chosen we would obtain π terms that can be reduced to the same value as when zero and 1 are chosen.

Let

$$c_3 = 1 \qquad c_6 = 0 \qquad c_9 = 0$$
$$c_4 = 0 \qquad c_7 = 0 \qquad c_{11} = 0$$
$$c_5 = 0 \qquad c_8 = 0$$

Substituting these values into equations (4), (5) and (6), and solving yields

$$F: \quad 0 = 0 + 0 + 0 + c_{10}$$

$$L: \quad 0 = c_1 + c_2 + 1 + 0 - 0 + 0 + 0 - 0 - 2c_{10} + 0$$

$$T: \quad 0 = -c_1 + c_{10} - 0$$

Therefore $c_1 = 0$, $c_{10} = 0$, $c_2 = -1$ and $c_3 = 1$

and

$$\pi_a = \frac{W}{D} \qquad (8)$$

Assigning the following different combination of values to the 8 unknowns:

$$c_3 = 0 \qquad c_6 = 0 \qquad c_9 = 0$$
$$c_4 = 1 \qquad c_7 = 0 \qquad c_{11} = 0$$
$$c_5 = 0 \qquad c_8 = 0$$

substituting into equations (4), (5) and (6) again and solving yields

$$F: \quad 0 = 0 + 0 + 0 + c_{10}$$

$$L: \quad 0 = c_1 + c_2 + 0 + 1 - 0 + 0 + 0 - 0 - 2c_{10} + 0$$

$$T: \quad 0 = -c_1 + c_{10} - 0$$

Therefore $c_{10} = 0$, $c_1 = 0$, $c_2 = 1$ and $c_4 = 1$

and

$$\pi_b = \frac{h}{D} \tag{9}$$

Assigning $c_5 = 1$ and the others zero and repeating the above solution we obtain another π term. We then assign $c_6 = 1$ and the others zero and solve for the next π term. This process is repeated until the last unknown (c_{11}) has been assigned the value 1.

Proceeding as above we obtain the following π terms.

$$\pi_a = \frac{W}{D} \qquad \pi_b = \frac{h}{D}$$

$$\pi_c = \frac{W}{V_{cr\text{-}d}\, D\mu} \qquad \pi_d = \frac{PD}{\mu V_{cr\text{-}d}}$$

$$\pi_e = \frac{b}{D} \qquad \pi_f = \frac{MHR}{D}$$

$$\pi_g = \frac{\rho D^2}{\mu V_{cr\text{-}d}} \qquad \pi_h = \frac{gD}{V_{cr\text{-}d}^2}$$

A general solution may be written as

$$\frac{gD}{V^2} = F\left(\frac{w}{D}, \frac{h}{D}, \frac{W}{VD\mu}, \frac{PD}{\mu V}, \frac{b}{D}, \frac{MHR}{D}, \frac{\rho D^2}{\mu V}\right) \tag{10}$$

The above dimensionless π terms can be rearranged as products, quotients or powers of each other to simplify them, and facilitate their use in our test program, without changing their validity.

We therefore let

$$\pi_1 = [\pi_h]^{-1} = \frac{V^2}{gD} \tag{11}$$

$$\pi_2 = [\pi_d][\pi_g]^{-1} = \frac{PD}{\mu V}\frac{\mu V}{\rho D^2} = \frac{P}{\rho D} \tag{12}$$

$$\pi_3 = \pi_b = \frac{h}{D} \tag{13}$$

$$\pi_4 = [\pi_c][\pi_g]^{-1} = \frac{W}{VD\mu}\frac{\mu V}{\rho D^2} = \frac{W}{\rho D^3} \tag{14}$$

$$\pi_5 = \pi_a = \frac{w}{D} \tag{15}$$

$$\pi_6 = [\pi_c][\pi_g][\pi_h]^{-1} = \frac{W}{VD\mu}\frac{\rho D^2}{\mu V}\frac{V^2}{gD} = \frac{\rho W}{\mu^2 g} \tag{16}$$

$$\pi_7 = \pi_e = \frac{b}{D} \tag{17}$$

$$\pi_8 = \pi_f = \frac{MHR}{D} \tag{18}$$

The general solution (10) may be rewritten as

$$\frac{V^2}{gD} = F\left(\frac{P}{\rho D}, \frac{h}{D}, \frac{W}{\rho D^3}, \frac{w}{D}, \frac{\rho W}{\mu^2 g}, \frac{b}{D}, \frac{MHR}{D}\right) \tag{19}$$

Due to experimental limitations and practical considerations some of the π terms were not varied in the test program. The π_8 term relating fluid density and viscosity was omitted since we are only concerned with tires hydroplaning on water, and for a narrow temperature range, where these variables may be considered as constants. The π_5 term was not varied due to the limited availability of similar tires having different section widths.

Modeling Theory

The relationships between model and prototype can, in general, be best established by the use of a series of equations which develop the scaling factor as a multiplier between measured model parameters and predicted prototype results. The following is the approach used in relating model tire hydroplaning to that of the full size tire. A more complete treatment of modeling theory can be found in reference 9. The approach below is usually called "Froude scaling."

If we chose scale factor λ to represent the ratio of model and prototype linear dimensions and the subscripts m and p to refer to model and prototype then basic geometric simulation is represented by

$$L_p = \lambda L_m \tag{20}$$

where every dimension in the model differs from the prototype by the factor λ.

If the density of model and prototype is to be identical (not always necessary but convenient), then

$$\frac{M_p}{L_p^3} = \frac{M_m}{L_m^3}$$

or

$$M_p = \lambda^3 M_m \tag{21}$$

For weights:

$$w = Mg$$

But gravity is constant for both model and prototype in this case. Therefore

$$W_p = M_p g = \lambda^3 M_m g = \lambda^3 W_m \tag{22}$$

From Newton's Law:

$$F_p = M_p A_p = \lambda^3 F_m = \lambda^3 (M_m A_m)$$

$$A_p = \lambda^3 \left(\frac{M_m}{M_p}\right) A_m = \lambda^3 \left(\frac{M_m}{\lambda^3 M_m}\right) A_m$$

therefore

$$A_p = A_m \tag{23}$$

Therefore accelerations in both the model and prototype are the same, and since

$$A = \frac{L}{T^2}$$

Therefore

$$\frac{L_p}{T_p^2} = \frac{L_m}{T_m^2}$$

$$T_p^2 = \frac{L_p}{L_m} T_m^2 = \lambda T_m^2$$

therefore

$$T_p = \sqrt{\lambda}\, T_m \tag{24}$$

i.e., events occur more rapidly with a scale model.

For velocities,

$$V = \frac{L}{T}$$

therefore

$$V_p = \frac{L_p}{T_p} = \frac{\lambda L_m}{\sqrt{\lambda}\, T_m} = \sqrt{\lambda}\, Vm \qquad (25)$$

For ground pressure or tire inflation pressure:

$$P = \frac{W}{L^2}$$

or

$$P_p = \frac{W_p}{L_p^2} = \frac{\lambda^3 W_m}{\lambda^2 P_m^2} = \lambda\, P_m \qquad (26)$$

i.e., the ground pressure or inflation pressure of a model should be less than that of the prototype.

Once the scaling relationship for the three primary units (weight, length, and time) have been obtained, any other parameter can be obtained by writing the equation in terms of its dimensions, then scaling each individual dimension and collecting terms. This is the method used to obtain the relationship for velocity and inflation pressure, equations (25) and (26).

MODEL

The model tires were fabricated of an open cell polyurethane foam and coated with several layers of an impervious paint formulation (urethane) specifically designed to withstand the high degree of flexure that would be experienced by the model tire under heavy load. This coating serves the dual purpose of protecting the open cell polyurethane tire from abrasion and also seals the porous surface.

The tire is of rectangular cross section having a diameter of 8 inches and a section width of 3.25 inches. The polyurethane foam density was varied so as to model the contact patch bearing pressure and load-deflection characteristics of a representative full scale type III aircraft pneumatic tire.[1] The model tire was constructed with a smooth surface (bald). In addition the tire was modified to have 4 and 8 ribs with a depth of 1/32, 2/32 and 3/32 inch. These ribs had a rib width to groove width ratio of unity (Figure 1).

An 8 inch diameter by 2.80 inch section width pneumatic tire was chosen for testing as it allowed us to vary the inflation pressure. This tire is a "General Jet-Rib," nylon cord, 4-ply tire (Figure 2). The tire is intended to model a 40-inch diameter aircraft tire. This will give us a scale factor (λ) of 5 based on the tire diameters.

APPARATUS

The "rolling road"[8] (Figure 3) consists of a flat table test section 8 feet long by 3 feet wide over which a cord reinforced with rubber conveyor belt is run. The rubber belt is stretched over a pair of 20 inch O. D. hollow cylindrical drums. Power is supplied by a 40 HP direct current motor and timing belt which drives one of the drums. The "idler" drum is slightly crowned to stabilize the belt and prevent it from "walking" off the pulley. The drive drum is rubber lagged with a herringbone groove pattern to prevent it from hydroplaning at high test speeds (a problem encountered with a previous smooth drive drum). The DC drive motor is capable of providing variable belt surface speeds of up to 6000 ft/min, by means of a motor generator set and a closed loop feedback system. Belt speed is measured by means of a DC tach generator mounted on the drive drum axle.

The rubber belt was used to simulate a smooth road surface. Latter testing involved bonding an abrasive cloth to the rubber belt surface to simulate a "rough" surface. The abrasive cloth was bonded to the belt in 4 inch wide by 2 foot long strips. This was necessary to avoid separation of the bond due to differential stretching of the belt as it passed over the drums.

In order to simulate a wet or flooded roadway the "rolling road" has a water supply system capable of laying a 12 inch wide film of water, of variable thickness, on the road at a synchronous speed. This system consists of a 25 horsepower centrifugal pump, piping, water nozzle, control valves, flow measuring instrumentation and a 500 gallon water reservoir. Water film thickness is fixed by adjusting a hinged plate at the discharge end of the nozzle (Figure 4). By inserting different rods of specific diameters into a recessed groove above the nozzle plate the opening may be adjusted for any required water film thickness. In order for the test tire not to see any relative motion between the water and road surface it is necessary to adjust the water flow rate to match the road speed and desired film thickness setting of the nozzle. From simple geometry and conservation of mass principles the following equation is obtained relating belt speed (V), film thickness (h), film width (w) and water flow rate (Q).

$$Q\ (\text{gal/min}) = 0.625\ V\ (\text{ft/min})\ w\ (\text{ft})\ h\ (\text{in})$$

or

$$Q = 0.625\ V\ h \qquad \text{where } w = 1 \text{ ft water film width}$$

Figure 5 is a plot of required water flow rate versus belt speed for synchronization, for various water film thicknesses. The water flow system is limited to a flow rate of 320 gallons per minute.

The test tire is mounted on a modified "Grumman Mohawk" aircraft nose wheel strut. The strut is attached to fixed ceiling rails by a pair of roller bearings. Longitudinal motion is prevented by a parallelogram linkage which is also capable of measuring drag force. The tire and lower portion of the strut are free to move vertically with respect to the fixed upper portion. To achieve minimum frictional drag in the vertical axis the tire and lower strut are separated by a bronze sleeve bushing which is rotated about its vertical axis by a small electric motor. This reduces the vertical friction to approximately 0.2 pounds.

The tire is counterbalanced and loaded by a pulley and weight assembly. Removing counterbalance weights increases the vertical load on the tire to a maximum attainable load of 120 pounds. Vertical deflection or heaving of the wheel assembly can be measured by a rotary potentiometer mounted to the upper strut and connected to the lower strut via a string. The rotational speed of the test wheel is measured by a DC tach generator which together with the signal from the road speed tach is displayed and recorded on a Sanborn pen recorder.

TEST PROGRAM

Polyurethane Tire

The test program consisted of determining the critical hydroplaning speed, both spin down and spin up, for an 8 inch diameter by 3.25 inch wide rectangular cross-section polyurethane tire. The load on the tire and water film thickness was varied to determine their effect on spin down/up speeds.

The tire was modified to have a ribbed tread pattern in order to determine the effects of tread depth and number of ribs. Tests were performed with an 8 rib and 4 rib tire having rib depths of 1/32, 2/32 and 3/32 of an inch. The ratio of rib width to groove width was maintained at unity for both tread configurations. The test conditions were identical to that of the bald tire in order to allow a comparison. Tire footprint measurements were taken for each combination of load and tire configuration.

The test conditions for each tire configuration are listed in Table 1.

Pneumatic Tire

In order to determine the effects of tire inflation pressure an 8-inch diameter by 2.80 inch cross section "General Jet-Rib" tire was selected. This pneumatic tire was tested in the bald and full tread condition on the

smooth road surface, for the full range of tire inflation pressure, tire load, and water film thickness. The rolling road surface was then modified to have a textured surface and the above test conditions repeated to investigate the effect of surface texture.

The test conditions for each tire configuration are listed in Table II. A listing of the test conditions in terms of dimensionless π groups is presented in Table III.

TEST PROCEDURE

The method of determining the spin down speed is basically a process of iteration and consists of the following steps.

1) The tire inflation pressure and wheel load are set.
2) A desired water film thickness is determined.
3) An estimate of the spin down speed is made based on experience.
4) The rolling road speed is set at a speed slightly below the estimated spin down speed.
5) The water flow is adjusted for synchronization and film depth at the estimated spin down speed utilizing the flow graph shown in Figure 5.
6) The road speed is increased in small increments until the recorder trace indicates a loss in wheel speed.
7) If the road speed determined in (6) differs from the estimated speed, a new estimate is made and steps (4) to (6) repeated.

The final value of spin down speed, which is when the wheel spins down at the estimated speed, is obtained from the pen recorder traces. This recorder is calibrated with a hand tachometer prior to each series of tests and periodically during the course of testing.

RESULTS

Polyurethane Tire

Footprint measurements of the tire contact patch area showed that, for the polyurethane tires there was no widening of the footprint with increasing load, rather the footprint increased in length in proportion to imposed load, maintaining a constant bearing pressure.

The results of the hydroplaning tests for the seven configurations of rib depth and number of ribs are shown graphically in Figures 6 to 21.

Figures 6 and 7 are graphs of spin down and spin up speeds versus load, with water film thickness as a parameter, for the bald tire. A comparison of the two graphs shows that the spin up speed or rolling restoration speed is considerably lower than the spin down speed, the difference being approximately 20 percent. The significance of this observation is that once spin down speed has been attained, or the vehicle brakes applied to initiate hydroplaning, the vehicle must then slow down approximately 20 percent before rolling restoration occurs. This deceleration requires considerable distance as the wheel has no traction and hence the brakes are ineffective. A comparison of the spin up/down data for the 8 rib and 4 rib tire, with 1/32, 2/32, or 3/32 inch tread depth, shows that the difference in speeds is generally 20 to 30 percent. This can be seen by comparing Figures 8 and 9, 10 and 11, and each of the following pair of curves up to Figures 18 and 19.

Figures 20 and 21 are log-log plots of spin down speed versus load for a water film thickness of 0.201 inch. Tire tread depth is a parameter. The hydroplaning inception speed is shown to increase exponentially with tread depth for both the 4 and 8 rib tire.

Figure 22 is a cross plot of Figures 20 and 21, on cartesian coordinates, of spin down speed versus tread dep with water film and wheel load held constant at 0.021 inch and 30 pounds. This graph illustrates the differences between the 8 rib and 4 rib tire as a function of tread depth. For very shallow tread depth there is little difference in spin down speed. However, as the tread depth is increased, the larger number of ribs is shown to be quite superior. The 8 rib tire has a considerably higher hydroplaning inception speed for deep ribs, the advantage decreasing to zero as both tires approach the bald condition. Since the rib area of both tires were the same, this difference cannot be attributable to differences in bearing pressure.

Figure 23 is a cross plot on log-log coordinates of the data shown in Figure 6. Here V_{cr-d} is plotted versus water film thickness (h) for the bald tire with a load of 30 pounds. From the slope of the line it can be seen that hydroplaning speed varies inversely as approximately the one-sixth power of the water film thickness.

Pneumatic Tire

The pneumatic tire was tested in four different configurations, namely:

1) Bald tire on smooth road surface.
2) Full tread depth (5 rib) on smooth surface.
3) Bald tire on rough road surface (150 grit).
4) Full tread depth tire on rough road surface.

The test conditions for all four configurations in terms of primary variables are shown in Table II. Table III lists the test conditions in terms of the dimensionless groups.

Configuration I - Bald Tire - Smooth Road

Measurement of hydroplaning inception speed was made for 277 different sets of test conditions. Measured test data for these sets are listed in Table IV. This data is plotted in terms of the corresponding dimensionless π terms listed in Table III in order to generate a prediction equation. Figure 24 is a plot of π_1 (V^2/gD) versus π_2 $(P/\rho D)$ on log-log coordinates with π_3 (h/D) as a parameter, π_4 $(W/\rho D^3)$ is held constant.

Since the data forms a family of straight lines, an equation of the form $\pi_1 = B\pi_2^{\,n}$ may be obtained for the lines where B = intercept and n = slope of the line.

From Figure 24 we obtain

$$\pi_1 = 29\ \pi_2^{\,.375} \qquad (27)$$

where $\bar{\pi}_3 = 0.00938$ and

$\bar{\pi}_4 = 2.166$

The value of the intercept "B" can be found by several methods. It is equal to the value of the "ordinate" when the "abscissa" is equal to one, or the equation $\pi_1 = B\pi_2^n$ can be solved for B by substituting a set of values of π_1 and π_2, and the value of n, from the straight line, into the equation.

Depending on the value of the axis the most convenient method of determining "B", the intercept, is used.

From Figure 25 which is a log-log plot of π_1 versus π_3 with $\bar{\pi}_2$ and $\bar{\pi}_4$ held constant at 69.28 and 2.166 we obtain the relationship

$$\pi_1 = 48\ \pi_3^{-.245} \tag{28}$$

From Figure 26 which is a log-log plot of π_1 versus π_4 with $\bar{\pi}_2$ and $\bar{\pi}_3$ held constant at 69.28 and 0.00938 we obtain the relationship

$$\pi_1 = 116\ \pi_4^{.311} \quad \text{for} \quad \pi_4 \leq 2.166 \tag{29}$$

and

$$\pi_1 = 133\ \pi_4^{.102} \quad \text{for} \quad \pi_4 \geq 2.166 \tag{30}$$

The curve in Figure 26 is composed of two straight lines and hence we have two regions of concern.

Equations (27), (28), (29) and (30) are combined according to the relationship[9]:

$$\pi_1 = \frac{F(\pi_2, \bar{\pi}_3, \bar{\pi}_4)\ F(\bar{\pi}_2, \pi_3, \bar{\pi}_4)\ F(\bar{\pi}_2, \bar{\pi}_3, \pi_4)}{[F(\bar{\pi}_2, \bar{\pi}_3, \bar{\pi}_4)]^2}$$

to yield

$$\pi_1 = 7.42\ \pi_2^{.375}\ \pi_3^{-.245}\ \pi_4^{.311} \quad \text{for} \quad \pi_4 \leq 2.166 \tag{31}$$

$$\pi_1 = 8.94\ \pi_2^{.375}\ \pi_3^{-.245}\ \pi_4^{.102} \quad \text{for} \quad \pi_4 \geq 2.166 \tag{32}$$

In terms of the primary input parameters, equations (31) and (32) become

$$\frac{V_{cr-d}^2}{gD} = 7.42 \left[\frac{P}{\rho D}\right]^{.375} \left[\frac{h}{D}\right]^{-.245} \left[\frac{W}{\rho D^3}\right]^{.311} \quad \text{for} \quad \left[\frac{W}{\rho D^3}\right] \leq 2.166 \tag{33}$$

and

$$\frac{V^2_{cr-d}}{gD} = 8.94 \left[\frac{P}{\rho D}\right]^{.375} \left[\frac{h}{D}\right]^{-.245} \left[\frac{W}{\rho D^3}\right]^{.102} \quad \text{for } \left[\frac{W}{\rho D^3}\right] \geq 2.166 \qquad (34)$$

Equation (33) gives predicted values of V_{cr-d} which have a maximum error of 14.8 percent and an average error of 3.7 percent when compared to the experimental data. Equation (34) has a maximum error of 14 percent and an average error of 3.7 percent in predicted V_{cr-d} versus experimental data.

Configuration 2 - Treaded Tire - Smooth Road

The treaded tire has five ribs with a rib depth of 3/32 inch. This tire was tested for 136 different sets of test conditions, each set corresponding to a similar test for configuration 1. The test data for this configuration is listed in Table V.

Figures 27, 28 and 29 are log-log plots of π_1 versus π_2 , π_3 , and π_4. The method of obtaining the component equations is similar to the previous configuration and yielded:

From Fig. 27 $\quad \pi_1 = 21.5\, \pi_2^{.517} \qquad (35)$

From Fig. 28 $\quad \pi_1 = 35\, \pi_3^{-.380} \qquad (36)$

From Fig. 29 $\quad \pi_1 = 164\, \pi_4^{.482} \quad \text{for } \pi_4 \leq 1.62 \qquad (37)$

$\pi_1 = 237\, \pi_4^{-.292} \quad \text{for } \pi_4 \geq 1.62 \qquad (38)$

The component equations are combined to yield:

$$\pi_1 = 2.94\, \pi_2^{.517}\, \pi_3^{-.380}\, \pi_4^{.482} \quad \text{for } \pi_4 \leq 1.62 \qquad (39)$$

$$\pi_1 = 4.24\, \pi_2^{.517}\, \pi_3^{-.380}\, \pi_4^{-.292} \quad \text{for } \pi_4 \geq 1.62 \qquad (40)$$

Or in terms of the primary input parameters

$$\frac{V^2_{cr-d}}{gD} = 2.94 \left[\frac{P}{\rho D}\right]^{.517} \left[\frac{h}{D}\right]^{-.380} \left[\frac{W}{\rho D^3}\right]^{.482} \quad \text{for } \left[\frac{W}{\rho D^3}\right] \leq 1.62 \qquad (41)$$

and

$$\frac{V^2_{cr-d}}{gD} = 4.24 \left[\frac{P}{\rho D}\right]^{.517} \left[\frac{h}{D}\right]^{-.380} \left[\frac{W}{\rho D^3}\right]^{-.282} \quad \text{for } \left[\frac{W}{\rho D^3}\right] \geq 1.62 \qquad (42)$$

Equation (41) exhibits a maximum error of 34 percent and an average error of 10.5 percent between predicted value of V_{cr-d} and test data. Equation (42) exhibits a maximum error of 19.7 percent and average error of 6.4 percent.

Configuration 3 - Bald Tire - Rough Road

The road roughness is obtained by bonding strips of 150 grit aluminum oxide cloth around the length of the belt.

Measurements of spin down speed were made for 90 different sets of test conditions, each set corresponding to a similar set in the configuration 1 and 2 series. The test data for this configuration is shown in Table VI.

Figures 30, 31 and 32 are log-log plots of π_1 versus π_2 , π_3 and π_4. The method of obtaining the component equations is similar to the previous configuration and yielded.

$$\text{From Fig. 30} \qquad \pi_1 = 23.2\, \pi_2^{.507} \qquad (43)$$

$$\text{From Fig. 31} \qquad \pi_1 = 26.8\, \pi_3^{-.438} \qquad (44)$$

$$\text{From Fig. 32} \qquad \pi_1 = 189\, \pi_4^{.106} \qquad (45)$$

The component equations are combined to yield

$$\pi_1 = 2.78\, \pi_2^{.508}\, \pi_3^{-.436} \qquad (46)$$

or in terms of primary input parameters

$$\frac{V^2_{cr-d}}{gD} = 2.78 \left[\frac{P}{\rho D}\right]^{.507} \left[\frac{h}{D}\right]^{-.438} \left[\frac{W}{\rho D^3}\right]^{.108} \quad (47)$$

Equation (47) exhibits a maximum error of 17.2 percent and an average error of 5.8 percent in V_{cr-d} when compared to our experimental data.

Configuration 4 - Treaded Tire - Rough Road

The objective of this series of tests was to generate sufficient data so as to be able to derive a prediction equation for this configuration. By varying the surface roughness it may have been possible to include a "roughness" factor in the prediction equations to account for surface texture. The speed limits and water flow limits of the rolling road apparatus were exceeded and only 9 data points generated. This data is listed in Table VII.

DISCUSSION

During the course of testing of the various tire configurations certain phenomena were observed which are worthy of comment.

The "bow wave" and forward splash would not always disappear when the wheel "spun down." It appears that the test conditions such as water film thickness, load, etc., have an influence. The forward splash and bow wave would disappear or be reduced under certain test conditions but not for other test conditions.

The wheel would spin down to a complete stop under certain test conditions (thick water films and a rough road surface) but generally slowed down to some "idle" speed. The initial deceleration of the wheel on spin down is usually quite rapid and on the order of 1000 feet per second for our 8-inch diameter wheel then decelerating at a reduced rate until its idle speed is reached. Once the wheel is "idling" in the spun down condition the idle speed

is independent of road speed. The wheel will continue to rotate at a fixed speed for any value of road speed provided we do not slow down below the rolling restoration speed.

When the test data on the 8" pneumatic tire, for various combinations of load, inflation pressure and water film thickness, are substituted into the prediction equations generated, the calculated value of spin down speed correlates well with the measured values.

The prediction equations for a bald tire operating on a smooth surface (Equations 33, 34) were compared to data published by Staughton[10] for a bald cross-ply tire. The film thickness, load, tire inflation pressure and wheel diameter (5.20-10) used by Staughton were inserted into Equation (33) and, the predicted values calculated, as well as the experimental values[10], plotted versus tire pressure in Figure 33. For reference, the values obtained from the equations for configurations 2 and 3 (treaded tire - smooth road and bald tire - rough road) are also shown. The Staughton data is for a bald cross ply 5.20-10 tire operating at a load of 500 pounds on a water film thickness of 0.374 inch. The correlation between the prediction equation and full size test data from Staughton is quite good.

The prediction equations for configurations 2 and 3 produce lines that are quite close together and higher in speed than that of configuration 1. This suggests that the drainage in the tire-road surface interface is similar for the treaded tire - smooth road and bald tire - rough road combinations.

These predictions do not agree completely with the widely accepted Horner-Dreher prediction[5] (plotted as a dashed line in Figure 33). Other researchers[11,12] also have found hydroplaning trends to be less than the square root of pressure found by Horner and Dreher (see the line of Staughton's[10] data, also plotted on Figure 33).

CONCLUSIONS

Polyurethane Tire

1) The spin-up speed was determined to be approximately 20 to 30 percent lower than the spin down speed for both the 4 rib and the 8 rib tire.

2) For very shallow tread depth there is little difference between a 4 rib and an 8 rib tire. As the tread depth is increased, the larger number of ribs is quite superior; i.e., higher spin down speed, for the same ratio of rib area to groove area (Figure 22).

3) Spin down speed varies inversely as approximately the one-sixth power of water film thickness, a fairly mild relationship.

4) Footprint measurements of the tire contact patch area show that the nominal contact patch bearing pressure remains, in effect, constant with increasing load. The footprint aspect ratio (length/width) changes, however, and it is believed that this is responsible for the change in slope of the spin down versus load curve.

Pneumatic Tire

1) The effect of tire inflation pressure is significant and approximately the same for both the treaded tire - smooth road and smooth tire - rough road combination. It is less significant for the smooth tire - smooth road combination, being only slightly more significant than the other variables. In all cases, V_{cr-d} increases with increasing tire inflation pressure.

2) The effect of water film thickness is more pronounced for the smooth tire - rough road and treaded tire - smooth road configurations than for the smooth tire - smooth road. In all cases, the spin down speed decreases with increasing water film thickness.

3) Spin down speed does not necessarily increase with wheel load (Equations 41, 42). Log-log plots of the spin down speed parameter versus the load parameter show two load regimes for the configurations 1 and 2. The spin down speed increases with increasing load up to some point (40 lb for the 8 inch diameter wheel) then either increases at a slower rate or decreases with further load (Figures 26 and 29).

4) The method of dimensional analysis combined with a systematic test program has resulted in data from which prediction equations can be, and have been generated. The equations correlate quite well with our test data for an 8 inch diameter wheel and published data for a 20 inch diameter tire (5.20-10).

RECOMMENDATIONS

1) A series of tests be performed using pneumatic tires having different tread depths in order to include this effect into one prediction equation.

2) A series of tests to extend the range of road surface roughness should be performed in order to develop a relationship between surface roughness and spin down speed.

3) A somewhat larger pneumatic tire (10-12 inch diameter) should be used for future testing so as to minimize distortions due to our inability to scale every variable simultaneously, and to reduce the effect of relatively large carcass stiffness on small diameter tires.

Davidson Laboratory
Stevens Institute of Technology
Castle Point Station
Hoboken, New Jersey, 07030

Table I

8" Diameter Polyurethane Model Tire Test Conditions

Smooth Tread Surface

(Spin Down and Spin Up Test Points)

Load W (lb)	Water Film Thickness h (in)				
	0.012	0.021	0.045	0.075	0.125
5	↓	↓	↓	↓	↓
10					
20					
30					
40					
50					

8 Ribs x 1/32 Inch Deep - Area Ratio 1:1

(Spin Down and Spin Up Test Points)

5	↓	↓	↓	↓	↓
10					
15					
20					
25					
30					
40					
50					
55					

Table I [Cont'd]

Load W (lb)	Water Film Thickness h (in) 0.012	0.021	0.045	0.075	0.125
8 Ribs x 2/32 Inch Deep (Spin Down and Spin Up Test Points)					
5					
10					
15					
20					
25					
30					
35					
40					
45					
50					
55					
8 Ribs x 3/32 Inch Deep (Spin Down and Spin Up Test Points)					
5					
10					
15					
20					
25					
30					
40					
50					

Table I [Cont'd]

Load W (lb)	Water Film Thickness h (in) 0.012	0.021	0.045	0.125
4 Ribs x 1/32 Inch Deep - Area Ratio 1:1				
(Spin Down and Spin Up Test Points)				
5	↓	↓	↓	↓
10	↓	↓	↓	↓
20	↓	↓	↓	↓
30	↓	↓	↓	↓
50	↓	↓	↓	↓
4 Ribs x 2/32 Inch Deep				
(Spin Down and Spin Up Test Points)				
5	↓	↓	↓	↓
10	↓	↓	↓	↓
20	↓	↓	↓	↓
30	↓	↓	↓	↓
50	↓	↓	↓	↓
4 Ribs x 3/32 Inch Deep				
(Spin Down and Spin Up Test Points)				
5	↓	↓	↓	↓
10	↓	↓	↓	↓
20	↓	↓	↓	↓
30	↓	↓	↓	↓
50	↓	↓	↓	↓
60	—	↓	↓	↓

Table II

Pneumatic Tire Hydroplaning Model Test Conditions
Dimensional Variables

p, lb/in^2	W, lb*	h, in
	Configuration (1) Bald Tire - Smooth Road	
5	5 → 90	.021, .045, .075, .125
10	5 → 100	" " " "
15	5 → 100	" " " "
20	5 → 120	" " " "
25	5 → 120	" " " "
30	5 → 110	.021, .075, .045
	Configuration (2) Treaded Tire - Smooth Road	
5	5 → 80	.045, .075, .125
10	5 → 90	"
15	5 → 100	"
20	5 → 120	"
25	5 → 120	.075, .125
	Configuration (3) Bald Tire - Rough Road	
15	5 → 90	.045, .075, .125
20	5 → 80	"
25	5 → 90	"
	Configuration (4) Treaded Tire - Rough Road	
15	5 → 35	.075
15	10 → 20	.125

*Vertical load applied in 5 lb increments 5 through 20 lb, and 10 lb increments 20 through 120 lb.

Table III

Test Conditions (Dimensionless Groups)

Configuration 1

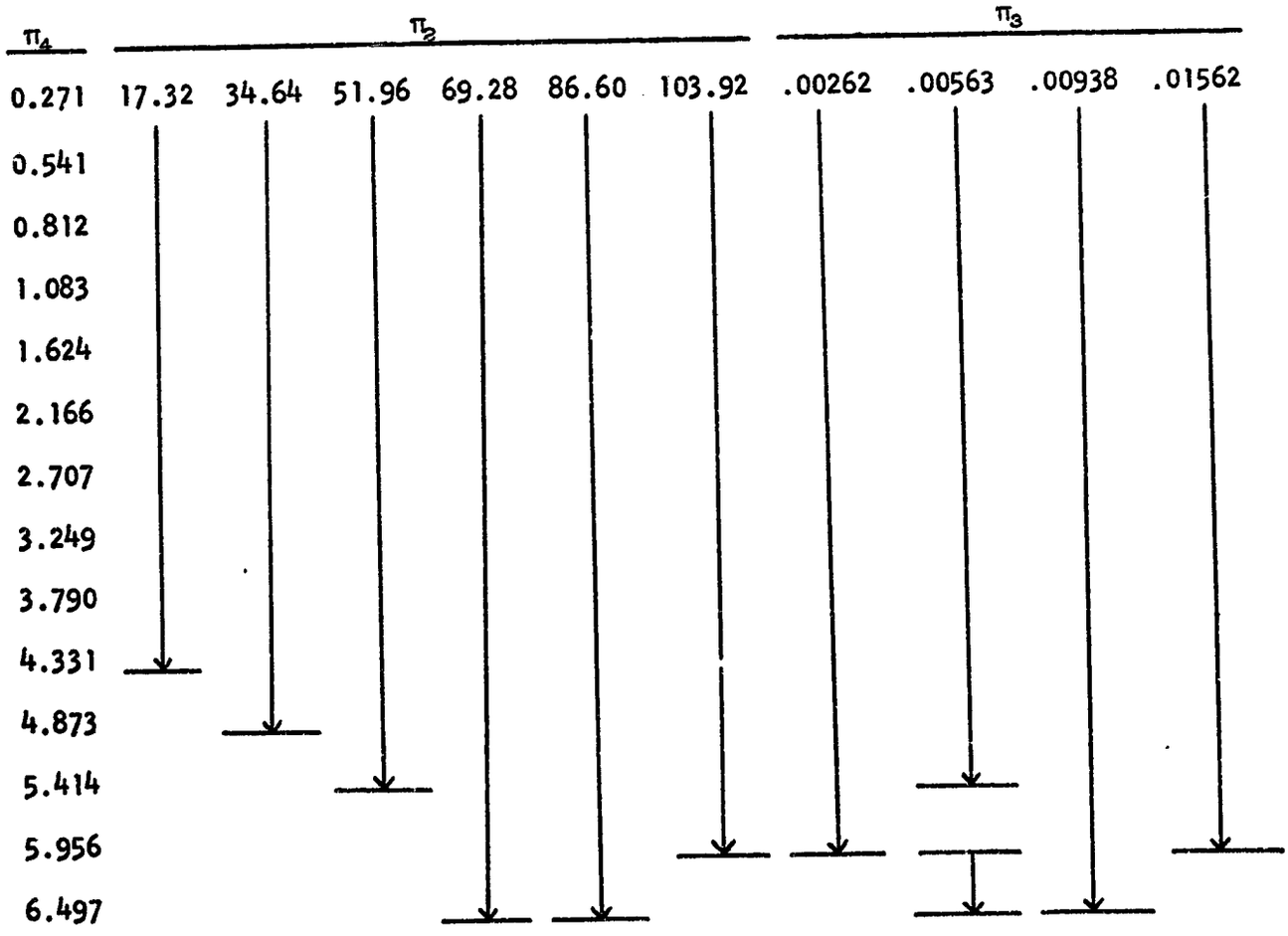

Note: $\pi_1 = \frac{V^2_{cr-d}}{gD}$ $\pi_2 = \frac{P}{\rho D}$ $\pi_3 = \frac{h}{D}$ $\pi_4 = \frac{W}{\rho D^3}$

$g = 115{,}776\ ft/min^2$ $\rho = 62.35\ lb/ft^3$ $D = 0.667\ ft$

Table III [Cont'd]

Configuration 2

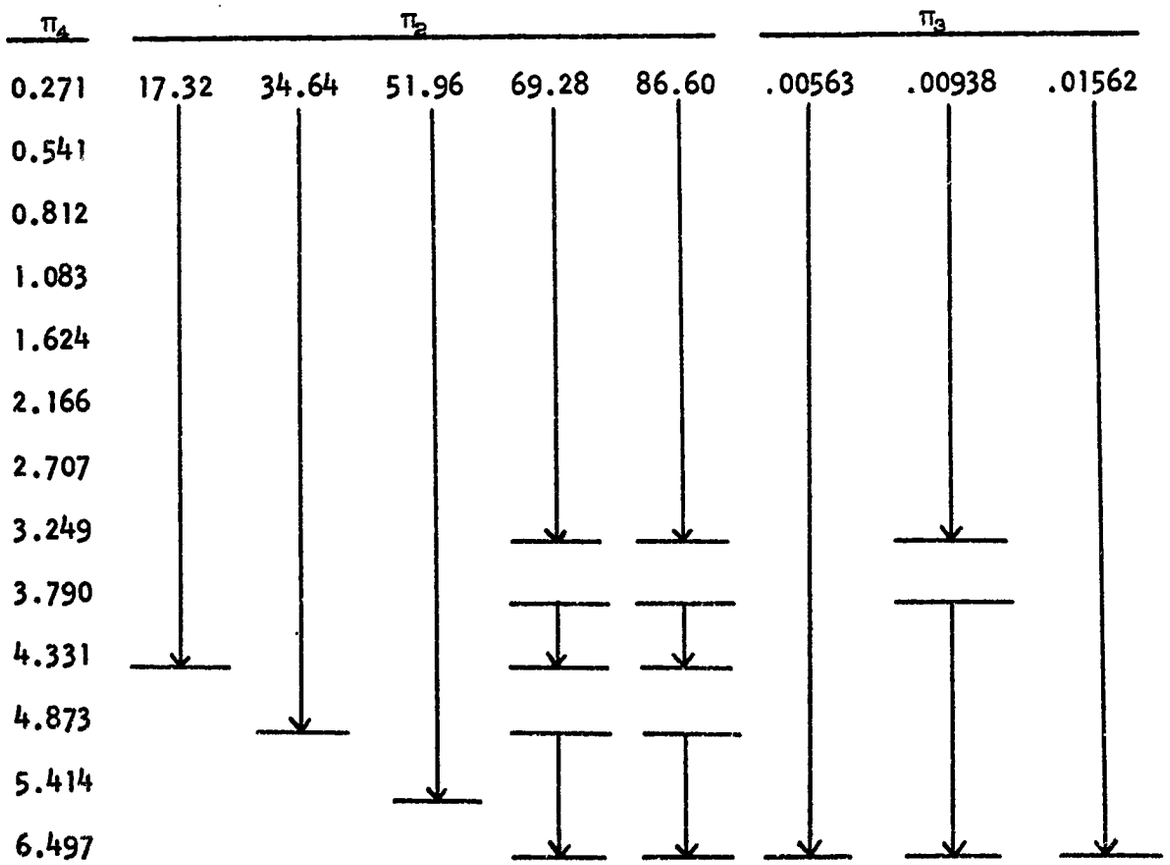

Table III [Cont'd]

Configuration 3

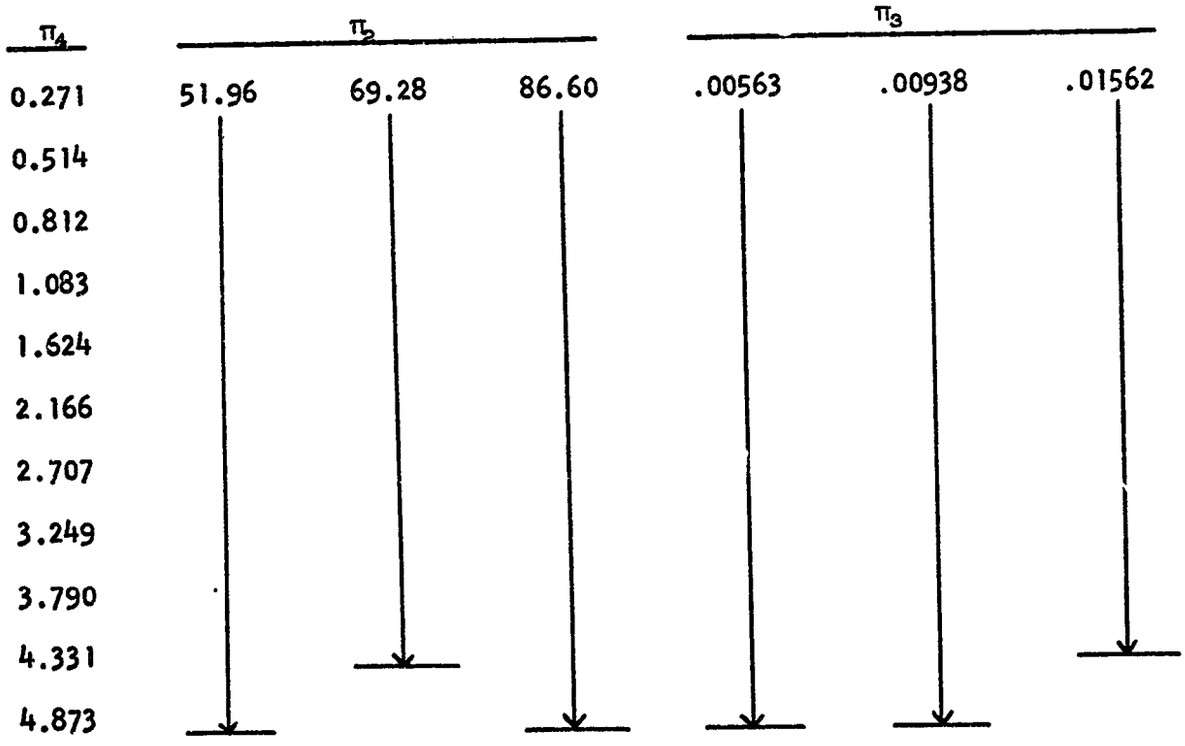

Configuration 4

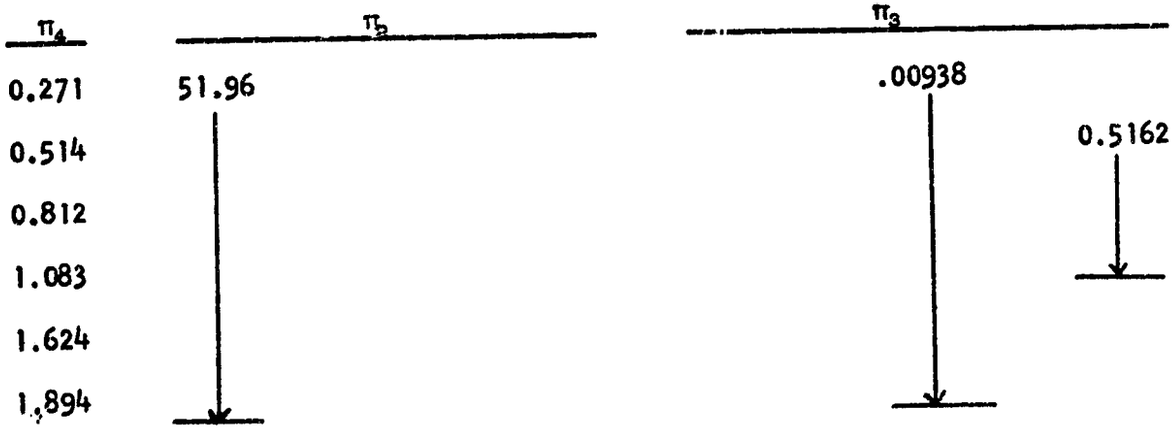

Table IV

Configuration 1 - Test Data

8" x 2.8" pneumatic tire, smooth tread,

smooth surface, 5 → 30 lb/in^2 tire inflation pressure

Water Film Thickness h (in)	Load W (lb)	Hydroplaning Speed V_{cr-d} (ft/min)					
		5 psi	10 psi	15 psi	20 psi	25 psi	30 psi
0.021	5	2000	1925	2300	2300	2450	2450
	10	2400	2400	2400	2500	2650	2650
	15	2500	2750	2600	2650	2775	2800
	20	2500	2925	2925	2900	3000	2950
	30	2750	2950	3200	3250	3400	3350
	40	2900	3100	3200	3350	3600	3625
	50	3050	3150	3200	3450	3700	3750
	60	3225	3225	3325	3525	3750	3800
	70	3550	3300	3250	3550	3900	3850
	80	3625	3425	3350	3525	3900	3900
	90	3700	3550	3350	3550	3950	3950
	100	-	3675	3500	3550	4050	4100
	110	-	-	-	3675	4200	4200
0.045	5	2200	2500	2600	2725	2875	-
	10	2600	2900	2900	2950	3100	-
	15	2675	3100	3150	3175	3250	-
	20	2750	3250	3400	3400	3550	-
	30	2900	3275	3475	3650	3700	-
	40	3100	3350	3500	3650	3800	-
	50	3250	3520	3550	3700	3725	-
	60	3300	3650	3625	3750	3675	-
	70	3300	3650	3650	3750	3750	-
	80	3350	3625	3700	3800	3800	-
	90	-	-	3725	3825	3825	-
	100	-	-	-	3825	3825	-
	120	-	-	-	3800	3850	-

Table IV [Cont'd]

Water Film Thickness h (in)	Load W (lb)	Hydroplaning Speed V_{cr-d} (ft/min)					
		5 psi	10 psi	15 psi	20 psi	25 psi	30 psi
0.075	5	1800	2100	2350	2450	2475	2700
	10	2100	2425	2650	2725	2775	2925
	15	2100	2800	2850	2850	2950	3050
	20	2300	2900	2950	3025	3100	3200
	30	2575	2800	3175	3300	3375	3450
	40	2850	2950	3175	3375	3525	3600
	50	2900	3050	3175	3350	3525	3600
	60	2925	3100	3200	3350	3550	3600
	70	2950	3200	3275	3400	3525	3575
	80	3050	3250	3325	3425	3550	3600
	90	-	3150	3400	3500	3600	3650
	100	-	-	3400	3525	3625	3650
	110	-	-	-	3550	3700	3700
	120	-	-	-	3575	3700	-
0.125	5	1775	2025	2175	2350	2375	2450
	10	1975	2375	2500	2650	2725	2800
	15	2075	2475	2600	2750	2850	2925
	20	2125	2525	2750	2925	2950	3050
	30	2325	2775	2950	3125	3225	3225
	40	2475	2700	3000	3225	3375	3275
	50	2625	2800	2900	3200	3450	3400
	60	2675	2775	2925	3125	3425	3525
	70	2725	2925	2950	3100	3400	3450
	80	2775	3000	3025	3100	3375	3450
	90	-	3050	3100	3150	3400	3500
	100	-	-	3125	3175	3400	3500
	110	-	-	-	3250	3400	3500

Table V

Configuration 2 - Test Data

8" x 2.8" pneumatic tire, 5 rib circumferential tread,

smooth surface, 5 → 25 lb/in^2 tire inflation pressure

Water Film Thickness h (in)	Load W (lb)	Hydroplaning Speed V_{cr-d} (ft/min)				
		5 psi	10 psi	15 psi	20 psi	25 psi
0.045	5	2600	3075	3100	3175	-
	10	3500	3525	3650	3675	-
	15	3575	3500	4000	3950	-
	20	3500	3750	4150	4275	-
	30	3400	3350	3900	4400	-
	40	3200	3500	3675	4100	-
	50	3050	3475	3750	3850	-
	60	2925	3200	3750	4150	-
	70	2750	3125	3500	-	-
	80	2675	3100	3350	3825	-
	90	-	-	3225	-	-
	100	-	-	-	3600	-
	120	-	-	-	3450	-
0.075	5	2550	2525	2600	2575	2675
	10	2850	2850	2900	2925	3100
	15	3150	3200	3225	3400	3375
	20	3050	3375	3500	3650	3650
	30	2925	3100	3525	4000	4050
	40	2925	3150	3250	3825	4150
	50	-	-	-	-	3825
	60	2700	2925	3300	3600	3775
	80	2550	2875	2975	3575	3825
	90	-	2825	-	-	-
	100	-	-	2800	3350	3600
	120	-	-	-	3200	3400

Table V [Cont'd]

Water Film Thickness h (in)	Load W (lb)	Hydroplaning Speed V_{cr-d} (ft/min)				
		5 psi	10 psi	15 psi	20 psi	25 psi
0.125	5	2100	2125	2225	2300	2350
	10	2450	2625	2725	2650	2750
	15	2700	2875	2900	2950	3075
	20	2825	3075	3100	3250	3300
	30	2750	3225	3500	3625	3750
	40	2850	3100	3275	3775	3950
	50	-	3200	-	3475	3975
	60	2700	-	3450	3500	3725
	70	-	3050	-	-	-
	80	2650	-	3200	3575	3800
	90	-	2975	-	-	-
	100	-	-	3100	3350	3700
	120	-	-	-	-	3500

Table VI

Configuration 3 - Test Data

8" x 2.8" pneumatic tire, smooth tread, #150 grit aluminum oxide surface, 15 → 25 psi tire inflation pressure

Water Film Thickness h (in)	Load W (lb)	Hydroplaning Speed V_{cr-d} (ft/min)		
		15 psi	20 psi	25 psi
0.045	5	4150	4300	4500
	10	4200	4400	4450
	15	4150	4300	4500
	20	4050	4050	4250
	30	4200	4200	4350
	40	4350	4550	4400
	50	4600	4600	4500
	60	4750	4700	4600
	70	4800	4800	4750
	80	-	4800	4800
	90	-	-	4900
0.075	5	3600	3700	4050
	10	3750	3900	4200
	15	3700	3950	4250
	20	3650	3850	4200
	30	3550	3750	4000
	40	3750	3800	4050
	50	3900	3900	4100
	60	4100	4000	4200
	70	4050	4125	4200
	80	4350	4300	4150
	90	4350	-	4200

Table VI [Cont'd]

Water Film Thickness h (in)	Load W (lb)	Hydroplaning Speed V_{cr-d} (ft/min)		
		15 psi	20 psi	25 psi
0.125	5	3300	3200	3350
	10	3450	3600	3550
	15	3500	3800	3750
	20	3400	3900	3900
	30	3300	3600	3950
	40	3400	3650	3800
	50	3600	3700	3850
	60	3650	3900	3900
	70	3775	4200	4150
	80	4100	-	-

Table VII

Configuration 4 - Test Data

8" x 2.8" pneumatic tire, 5 rib circumferential tread,

#150 aluminum oxide surface

Water Film Thickness h (in)	Load W (lb)	Hydroplaning Speed V_{cr-d} (ft/min) 15 psi	20 psi	25 psi
0.075	5	3750	-	-
	10	4350	-	-
	15	4600	-	-
	20	4900	-	-
	25	-	-	-
	30	5350	-	-
	35	5600	Note 1: Any further increase in load or inflation pressure, or decrease in film thickness will cause road to exceed maximum safe speed.	
	40	-		
	50	-		
	60	-		
0.125	5	-	-	-
	10	3850	-	-
	15	4150	-	-
	20	4300	Note 2: 4300 ft/min road speed requires a water flow rate of 327 GPM which is maximum equipment capability. Any further increase in W or P will cause road speed to increase beyond water flow capability.	
	25	-		
	30	-		
	35	-		
	40	-		
	50	-		
	60	-		

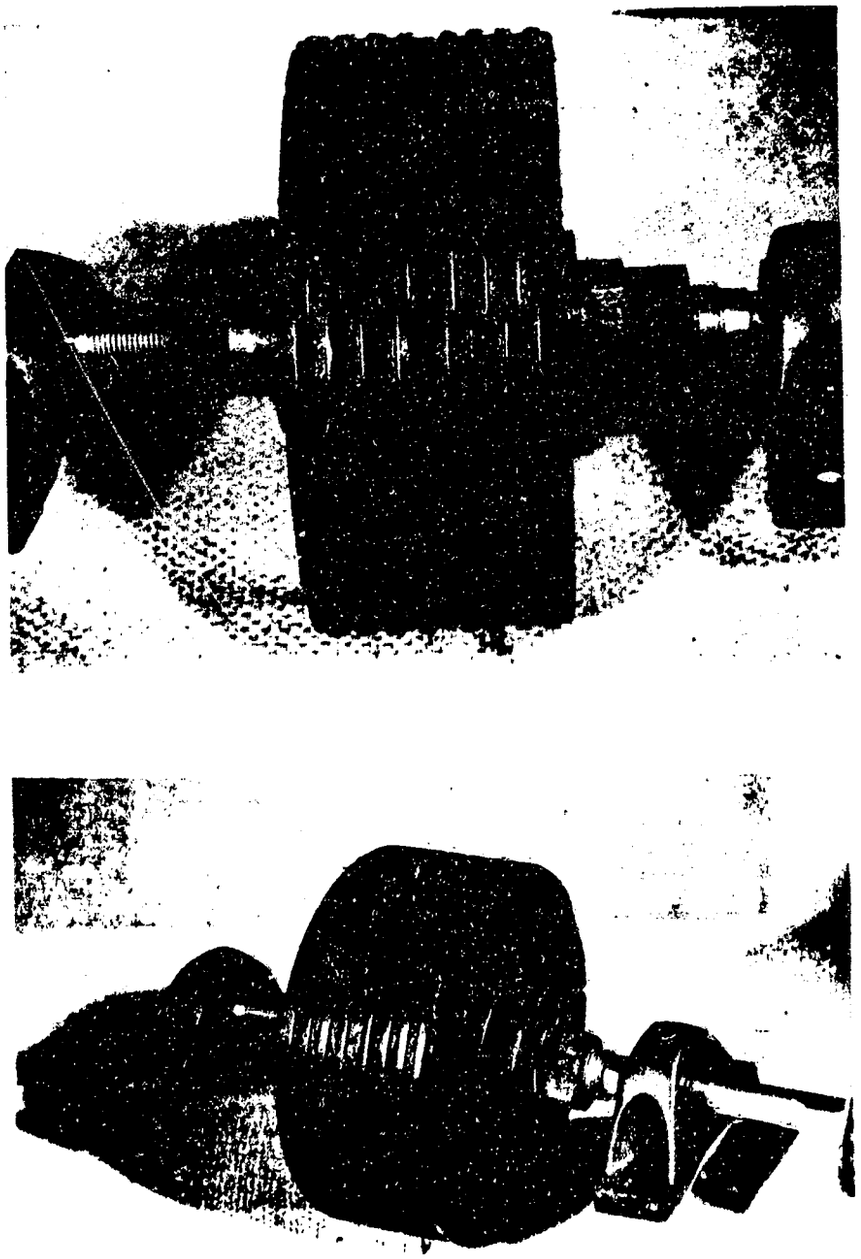

FIGURE 1. 8" DIA. x 3.25" WIDE POLYURETHANE TIRE (8 RIBS)

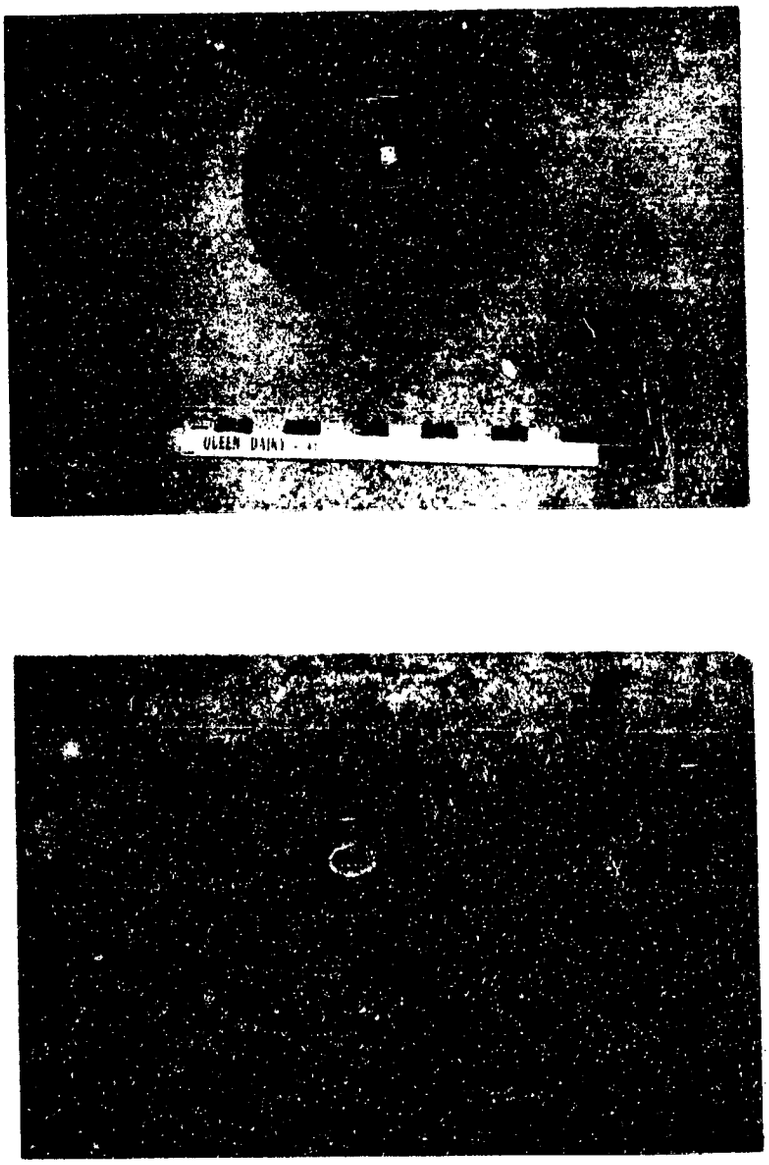

FIGURE 2. 8" DIA. x 2.80" PNEUMATIC NYLON CORD 4-PLY TIRE (SMOOTH AND FULL TREAD CONFIGURATION)

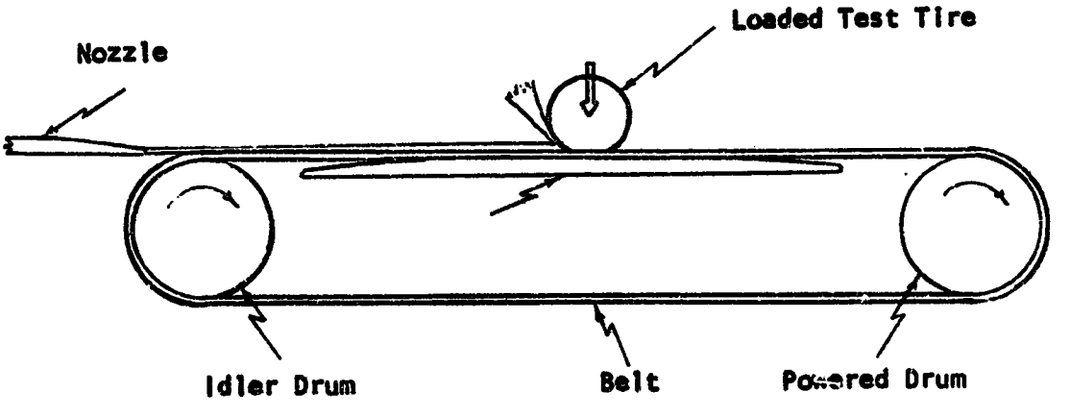

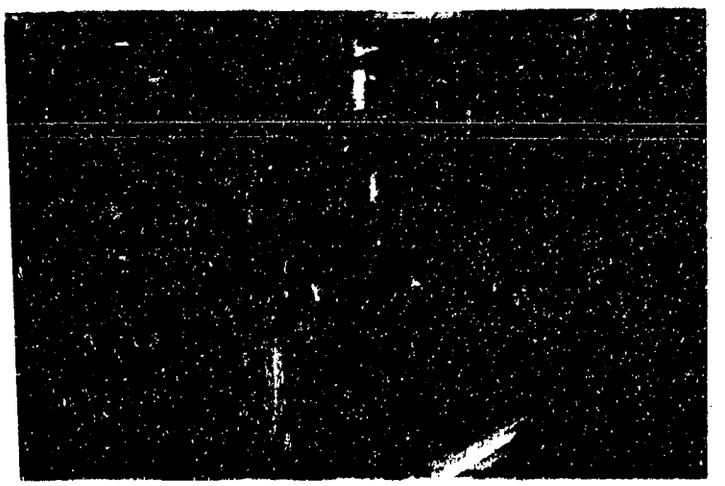

FIGURE 3. ROLLING ROAD

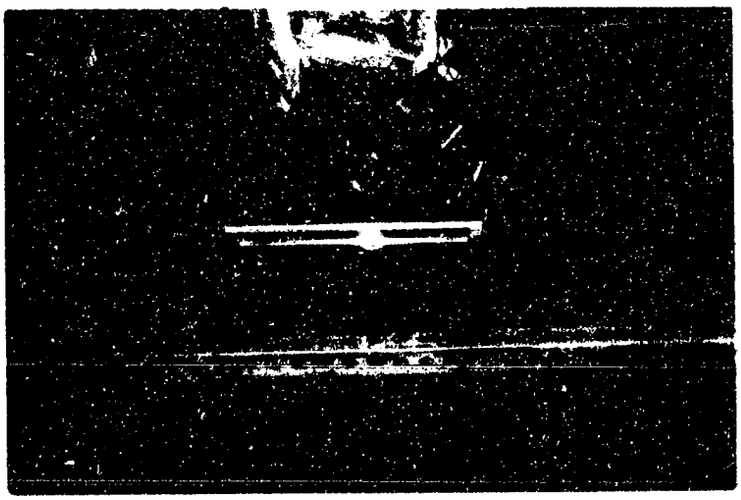

FIGURE 4. WATER FILM NOZZLE
(Variable Film Thickness by
Changing Spacer Rods at Dis-
Charge End)

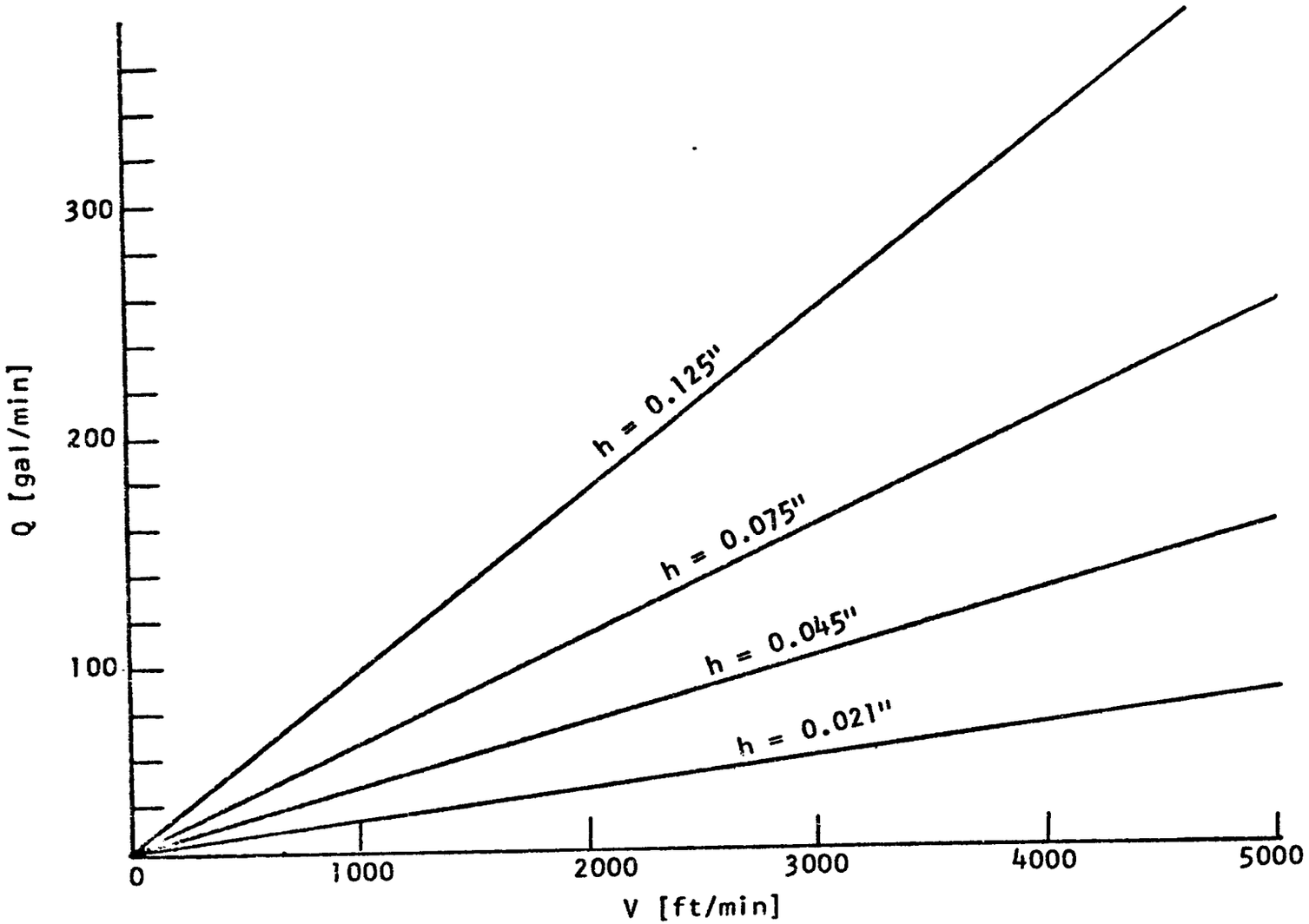

FIGURE 5. WATER FLOW RATE VS. BELT SPEED

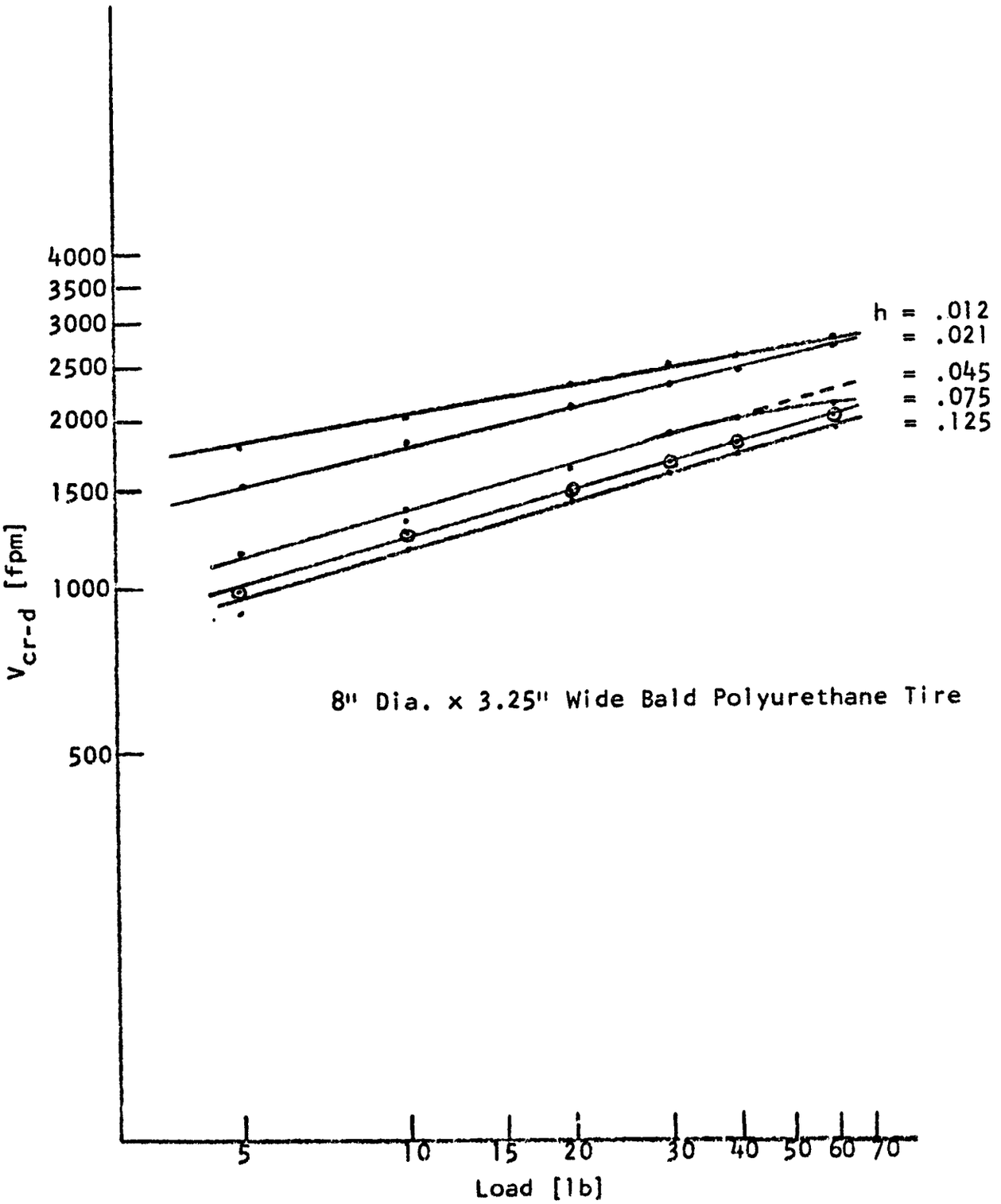

FIGURE 6. SPIN DOWN SPEED VS. LOAD (WATER FILM THICKNESS AS A PARAMETER)

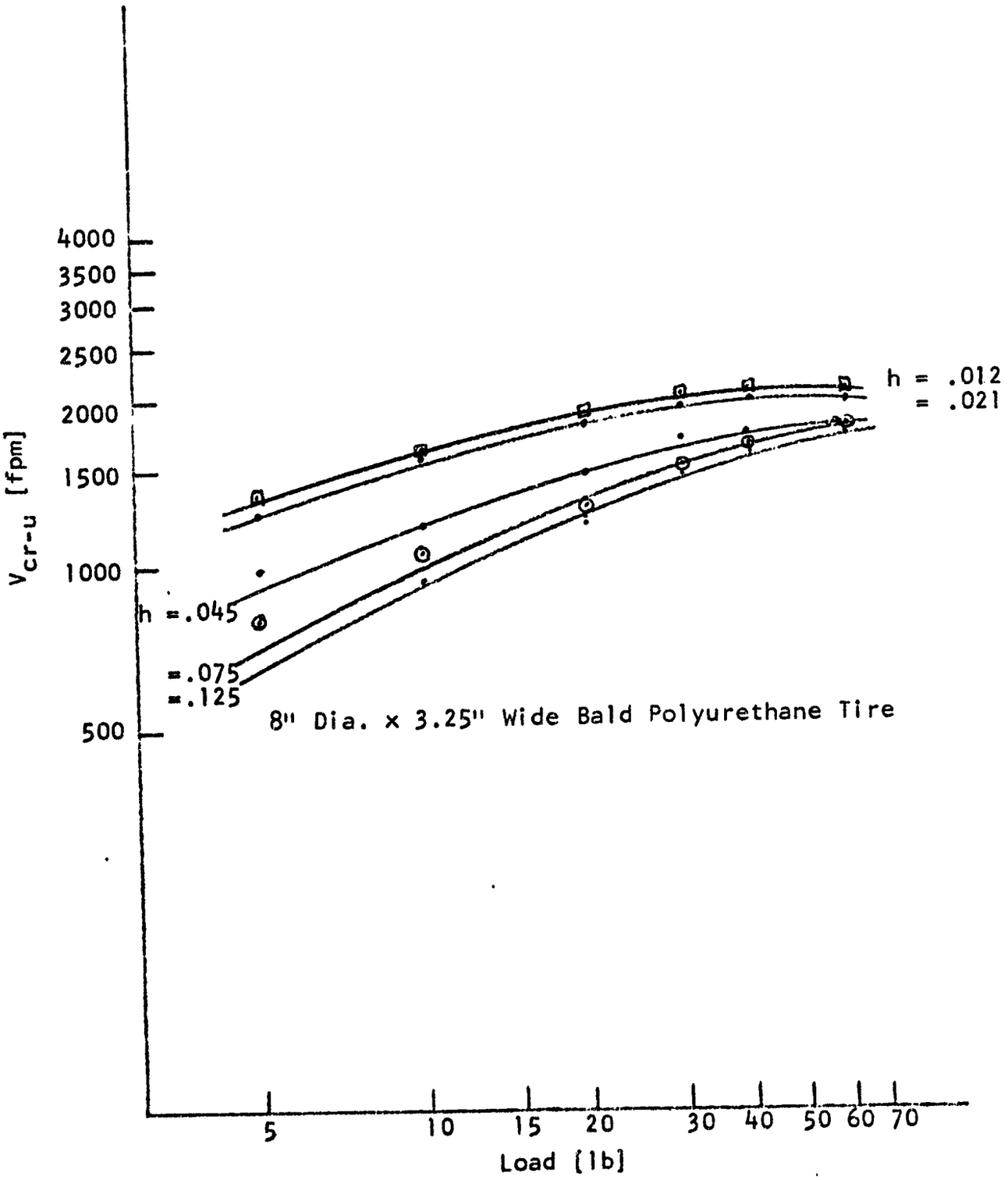

FIGURE 7. SPIN UP SPEED VS. LOAD (WATER FILM THICKNESS AS A PARAMETER)

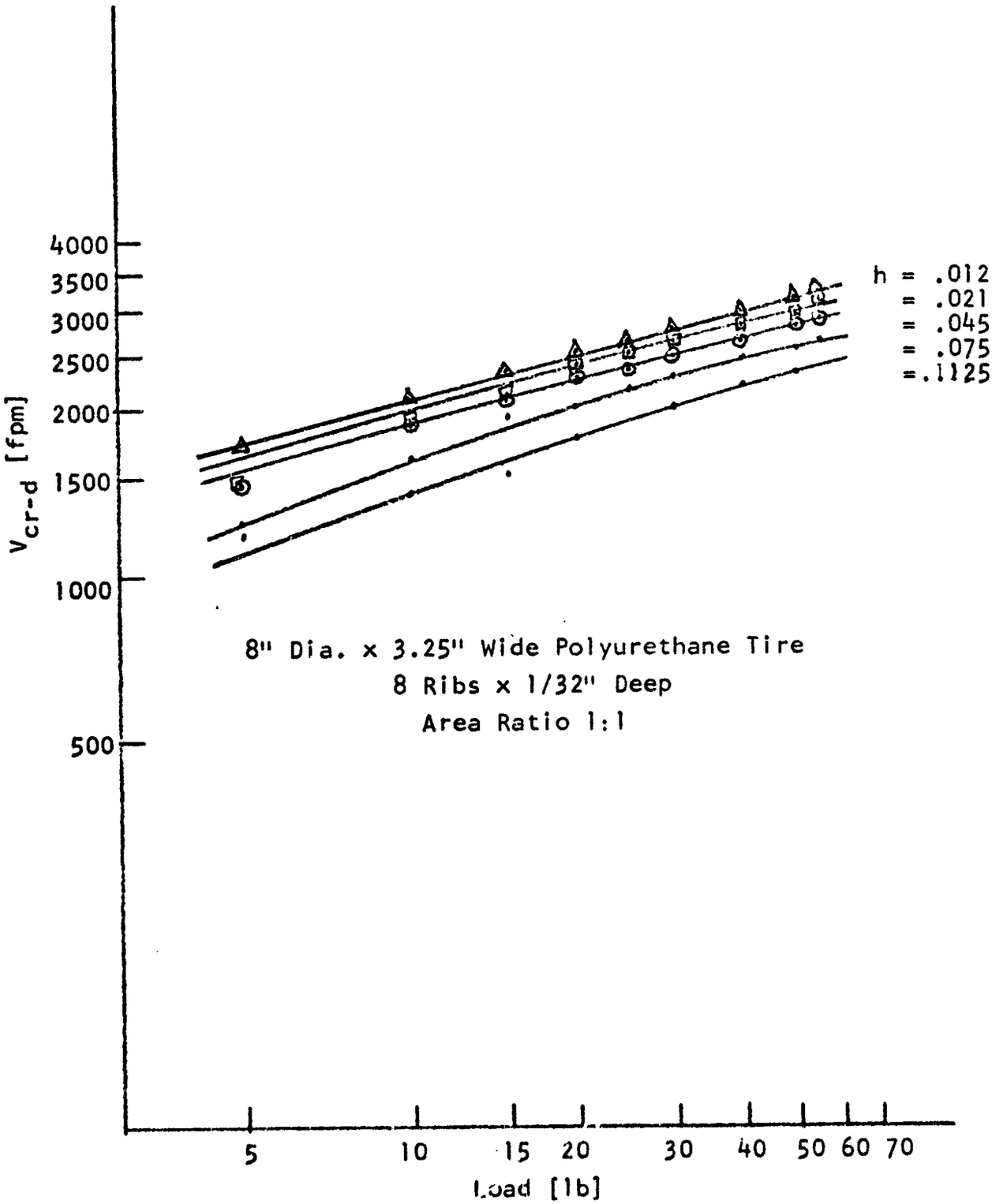

FIGURE 8. SPIN DOWN SPEED VS. LOAD (WATER FILM THICKNESS AS A PARAMETER

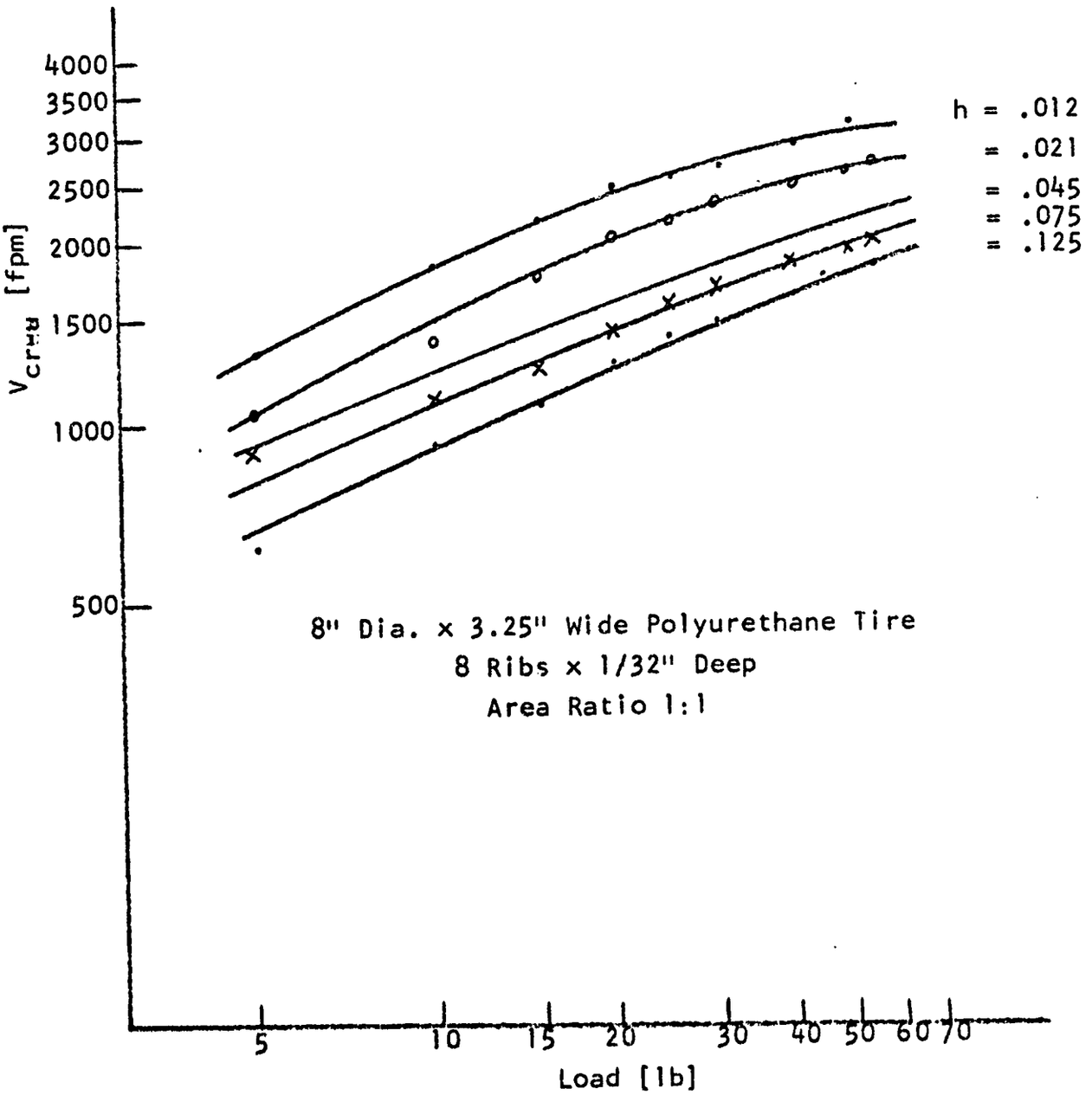

FIGURE 9. SPIN UP SPEED VS. LOAD (WATER FILM THICKNESS AS A PARAMETER)

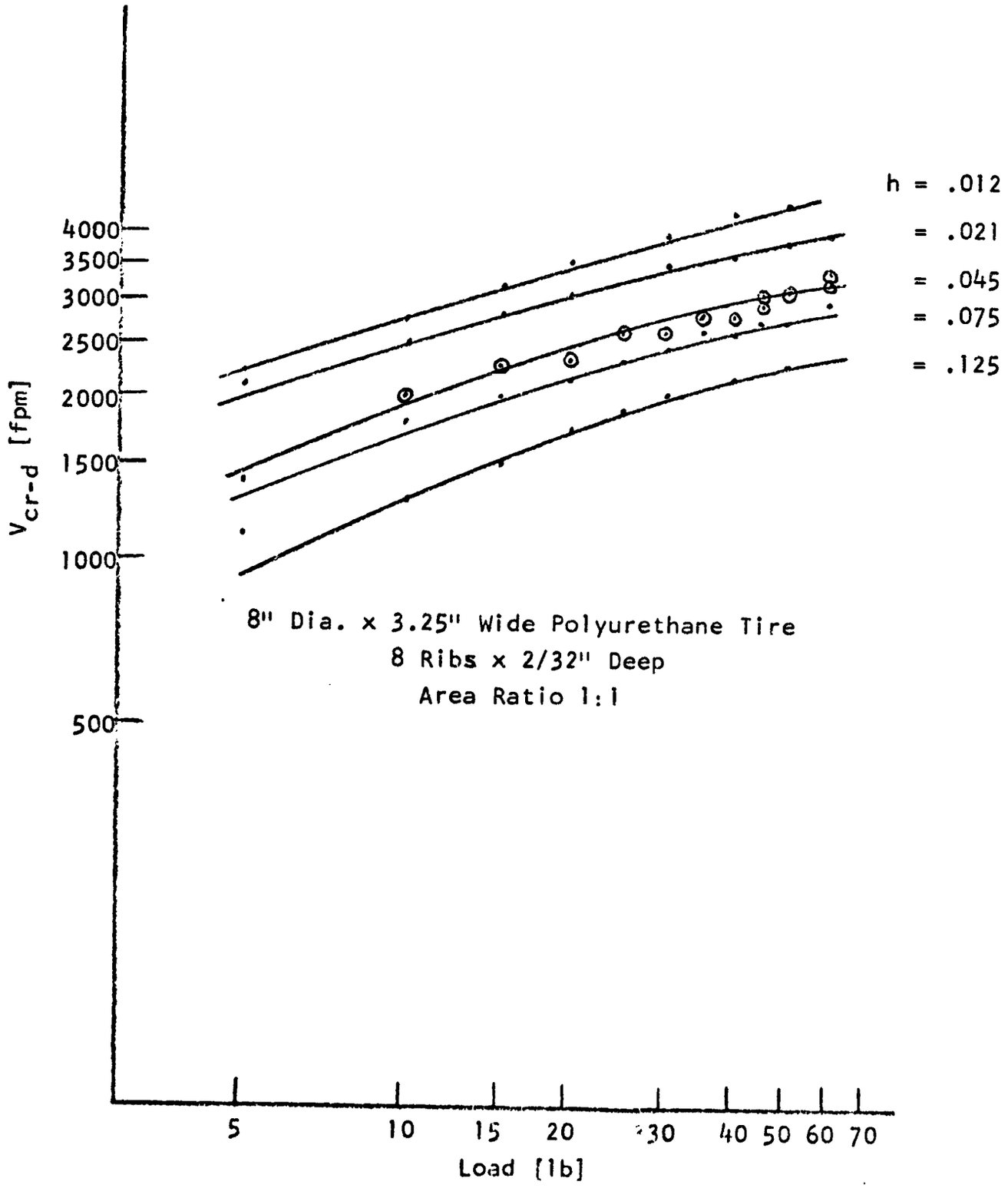

FIGURE 10. SPIN DOWN SPEED VS. LOAD (WATER FILM THICKNESS AS A PARAMETER)

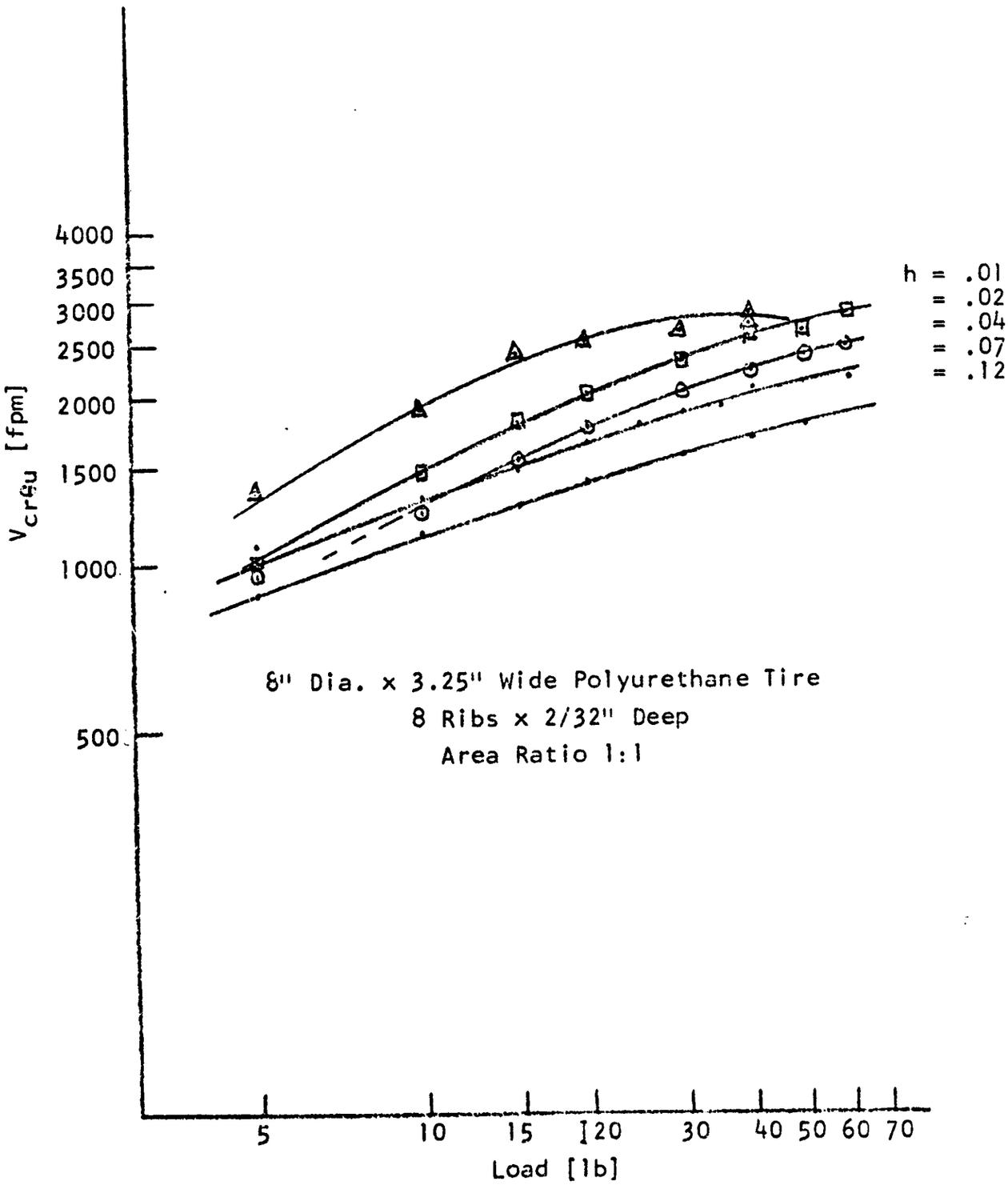

FIGURE 11. SPIN UP SPEED VS. LOAD (WATER FILM THICKNESS AS A PARAMETER)

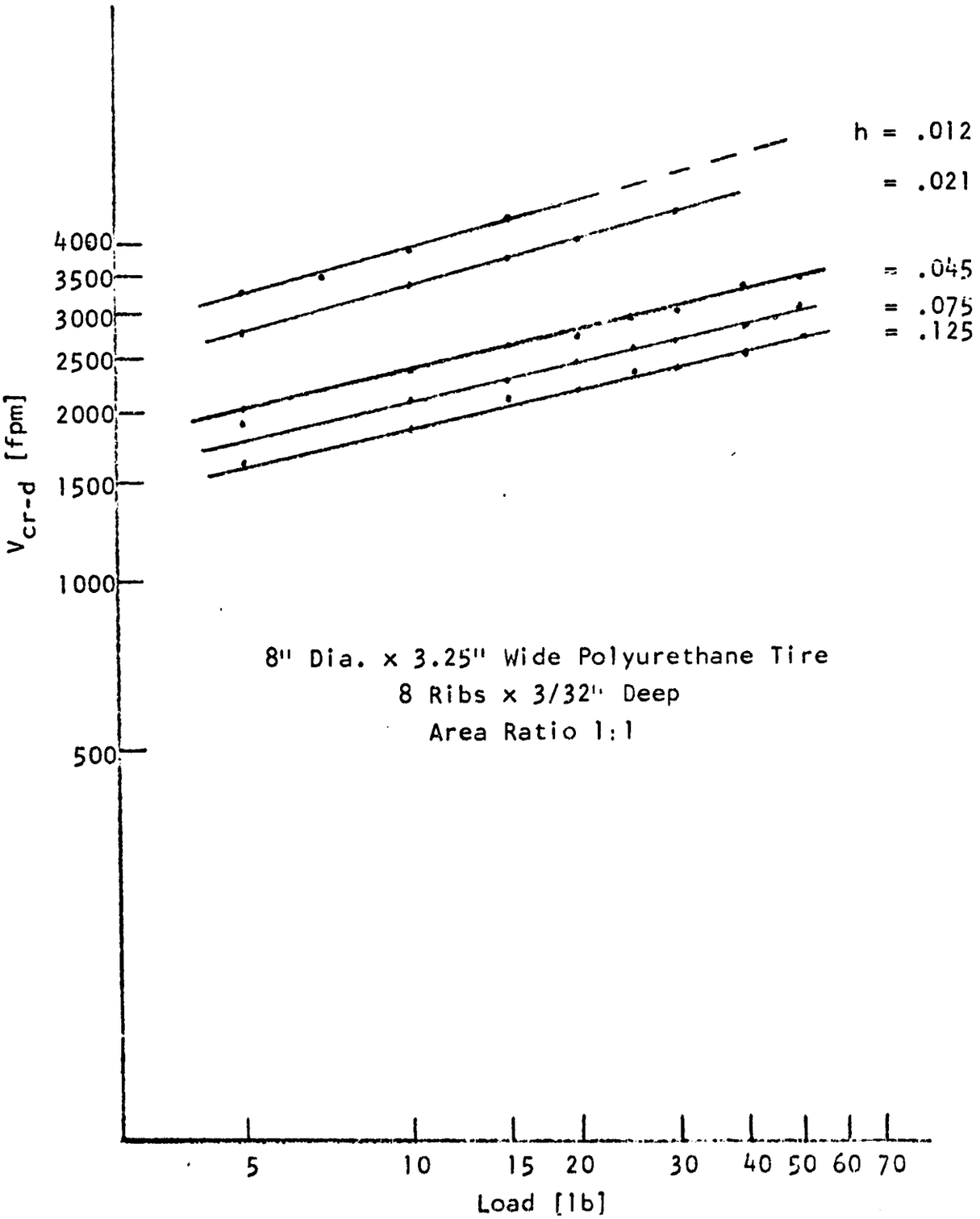

FIGURE 12. SPIN DOWN SPEED VS. LOAD (WATER FILM THICKNESS AS A PARAMETER)

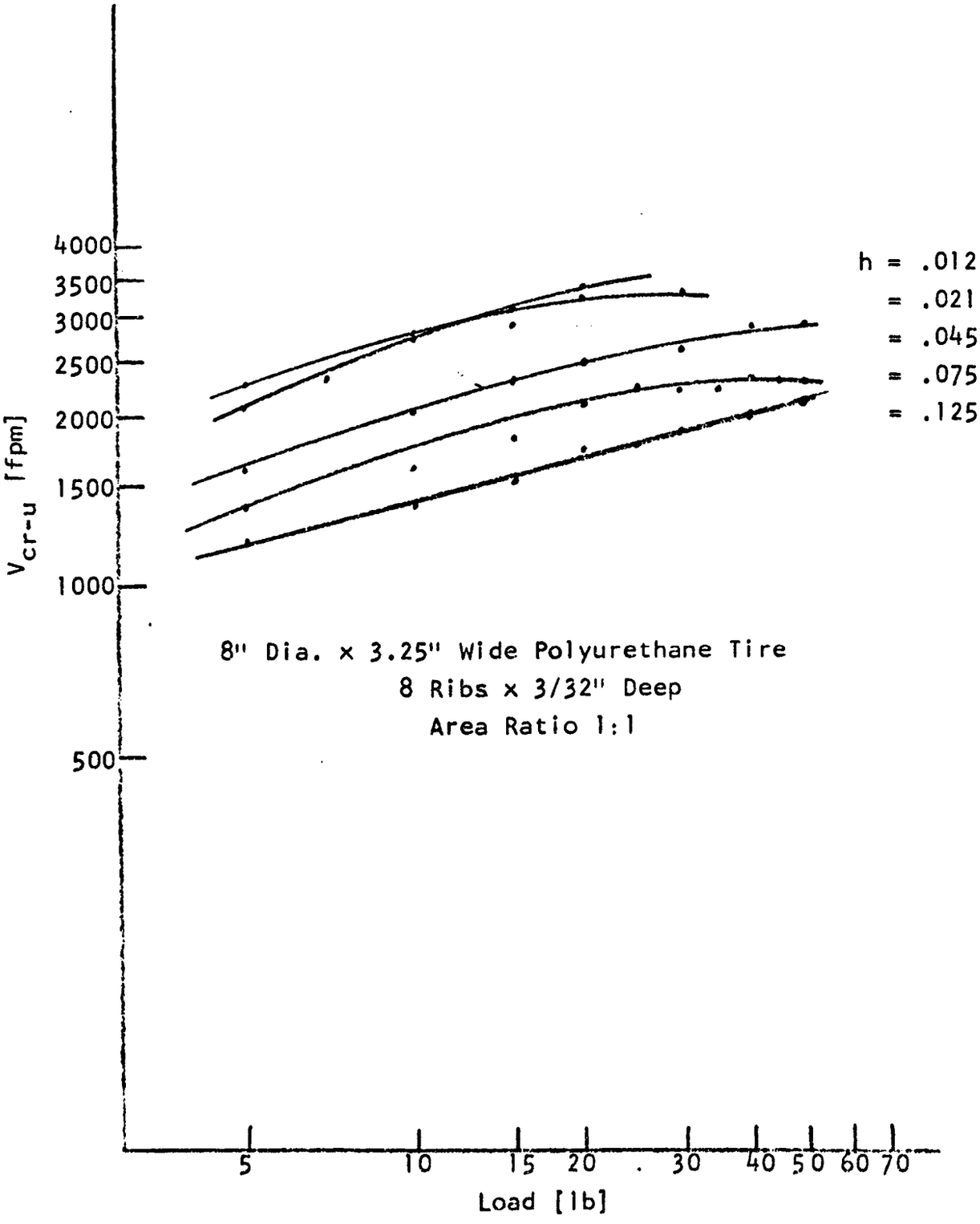

FIGURE 13. SPIN UP SPEED VS. LOAD (WATER FILM THICKNESS AS A PARAMETER)

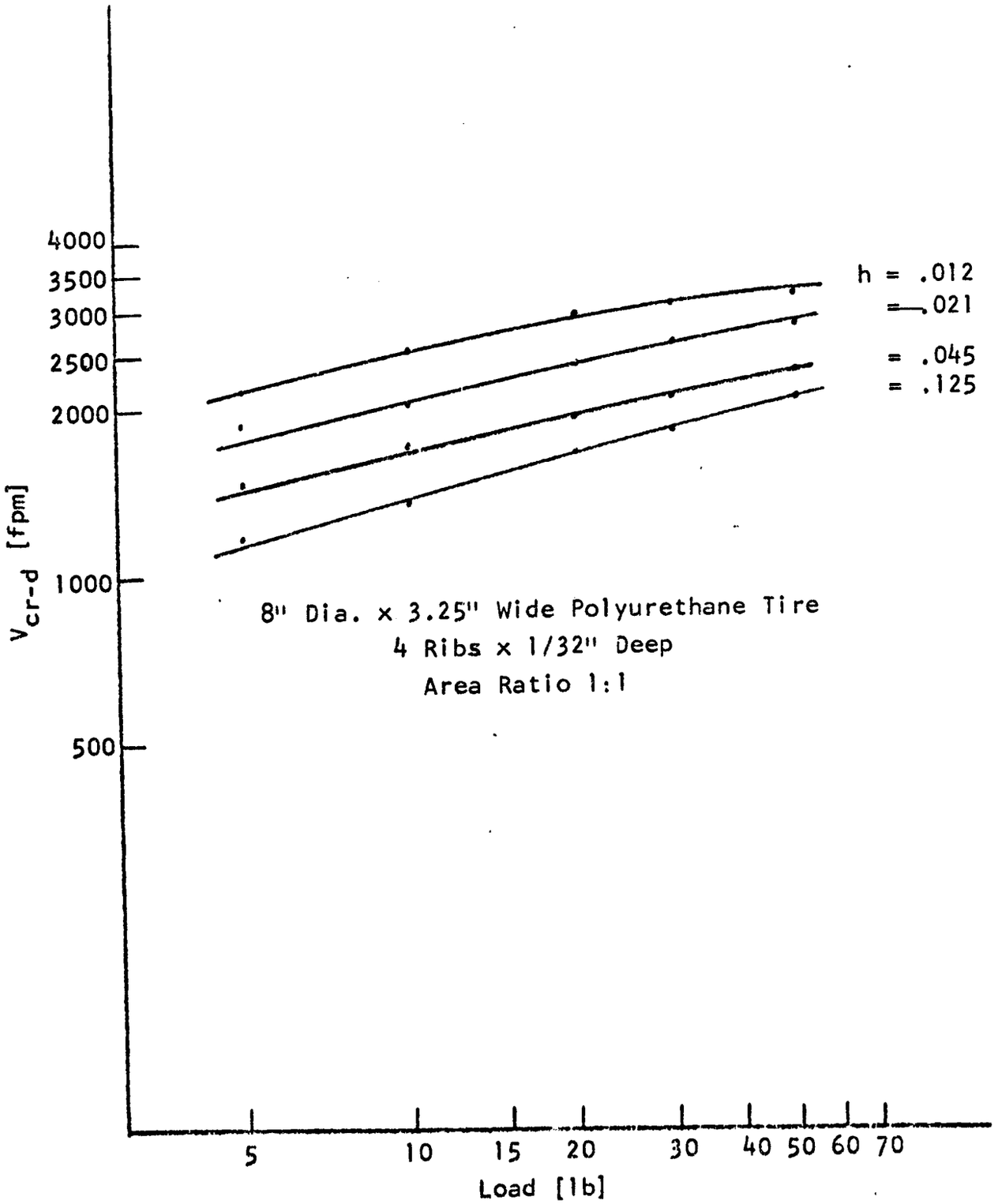

FIGURE 14. SPIN DOWN SPEED VS. LOAD (WATER FILM THICKNESS AS A PARAMETER)

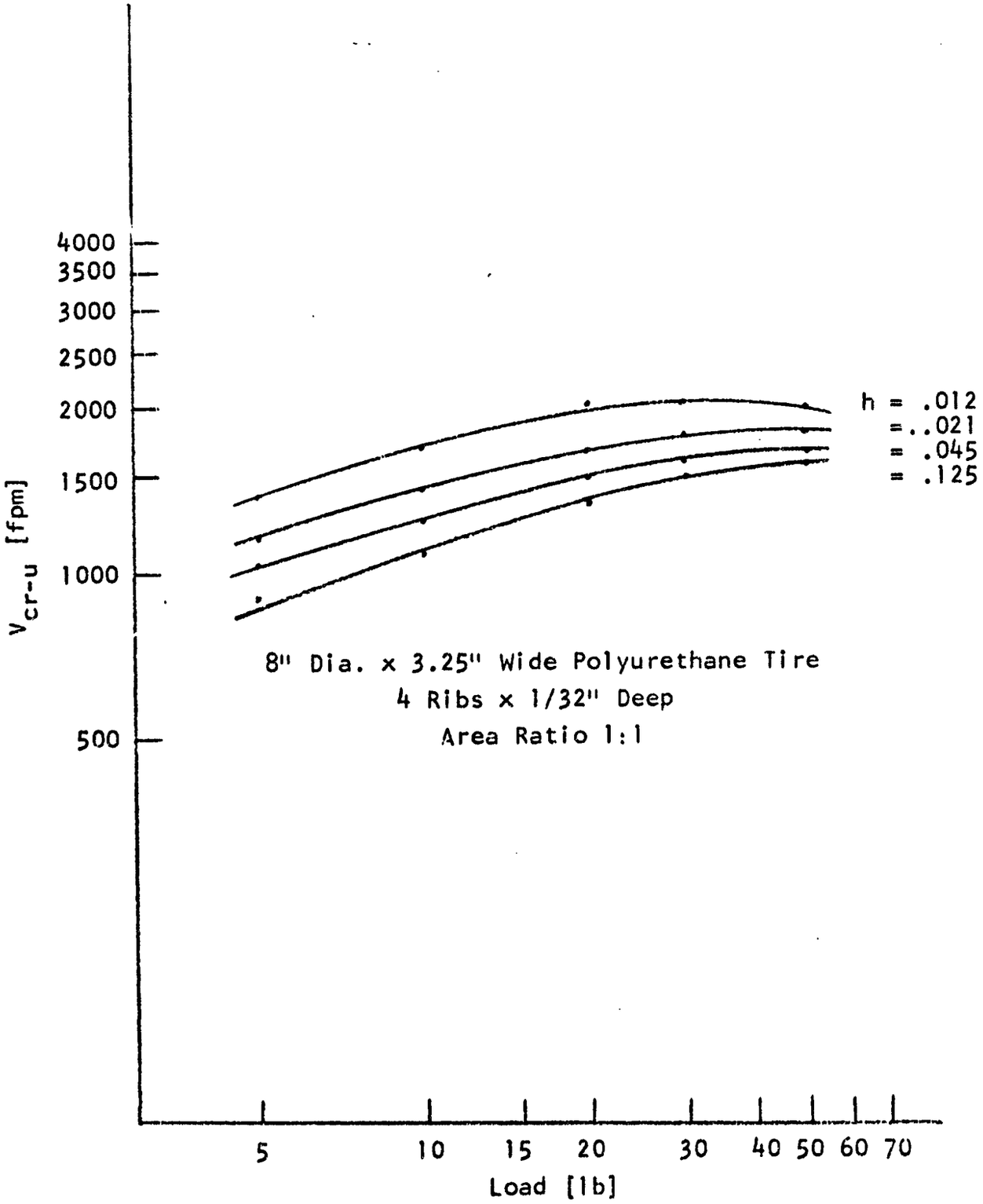

FIGURE 15. SPIN UP SPEED VS. LOAD (WATER FILM THICKNESS AS A PARAMETER)

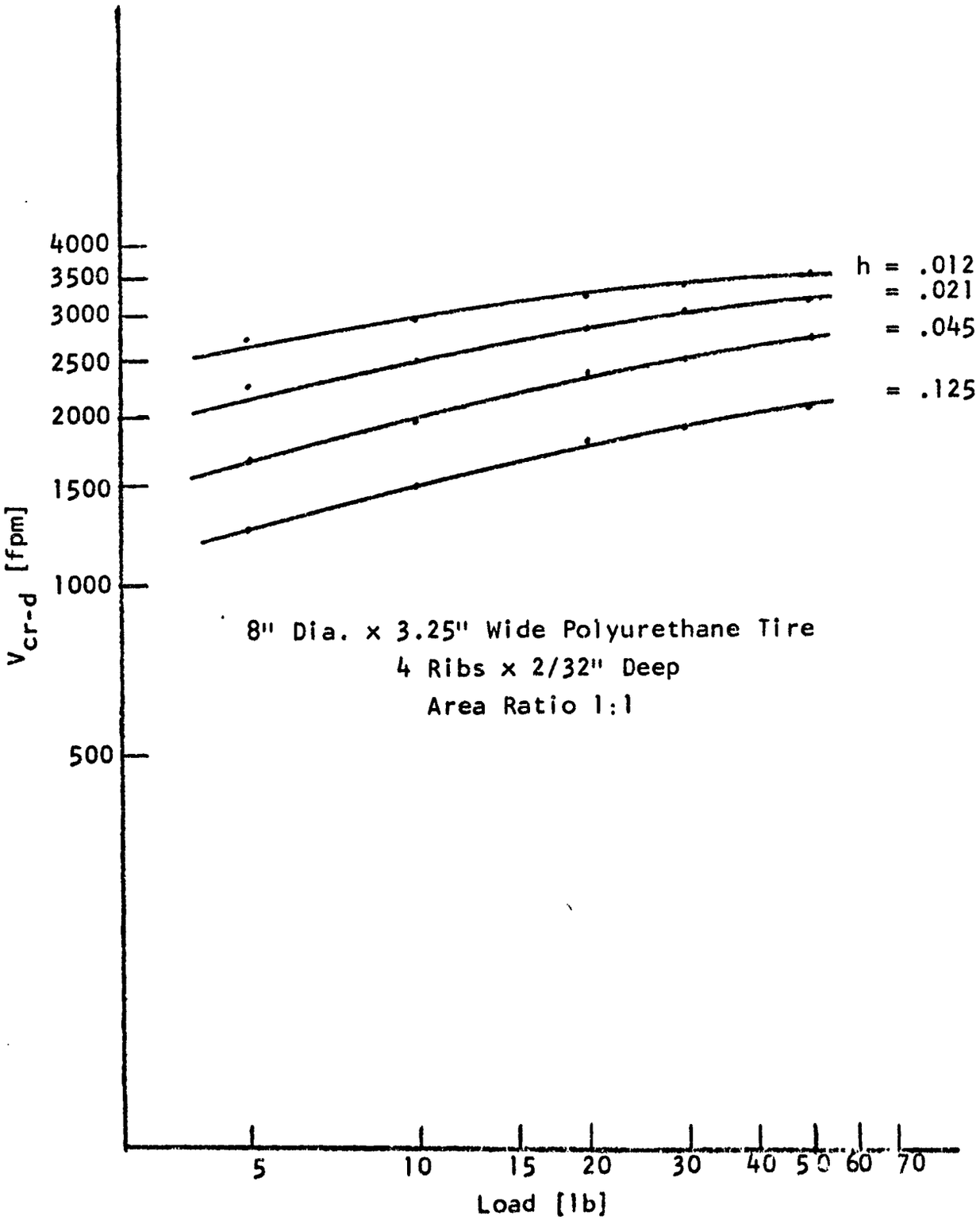

FIGURE 16. SPIN DOWN SPEED VS. LOAD (WATER FILM THICKNESS AS A PARAMETER)

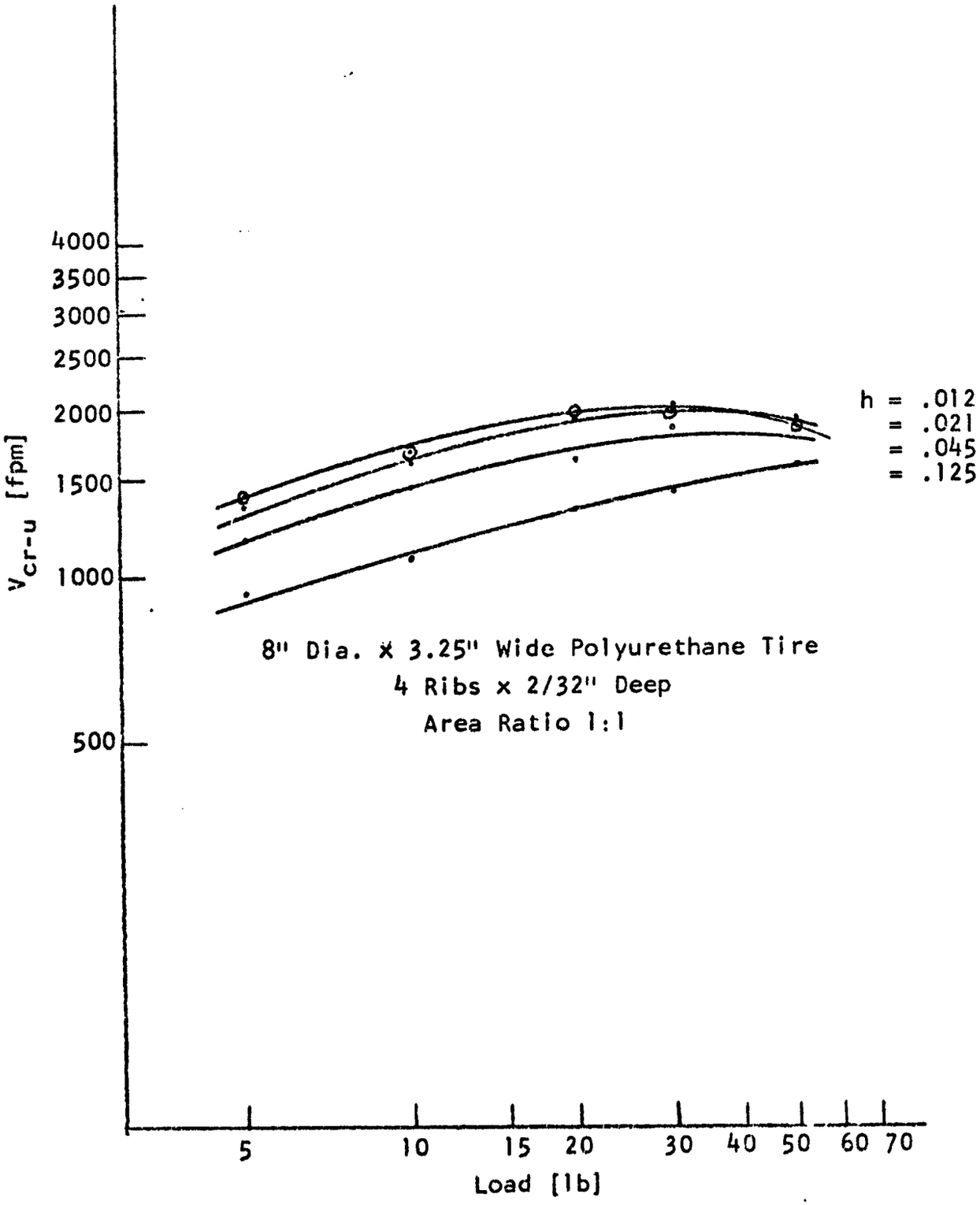

FIGURE 17. SPIN UP SPEED VS. LOAD (WATER FILM THICKNESS AS A PARAMETER)

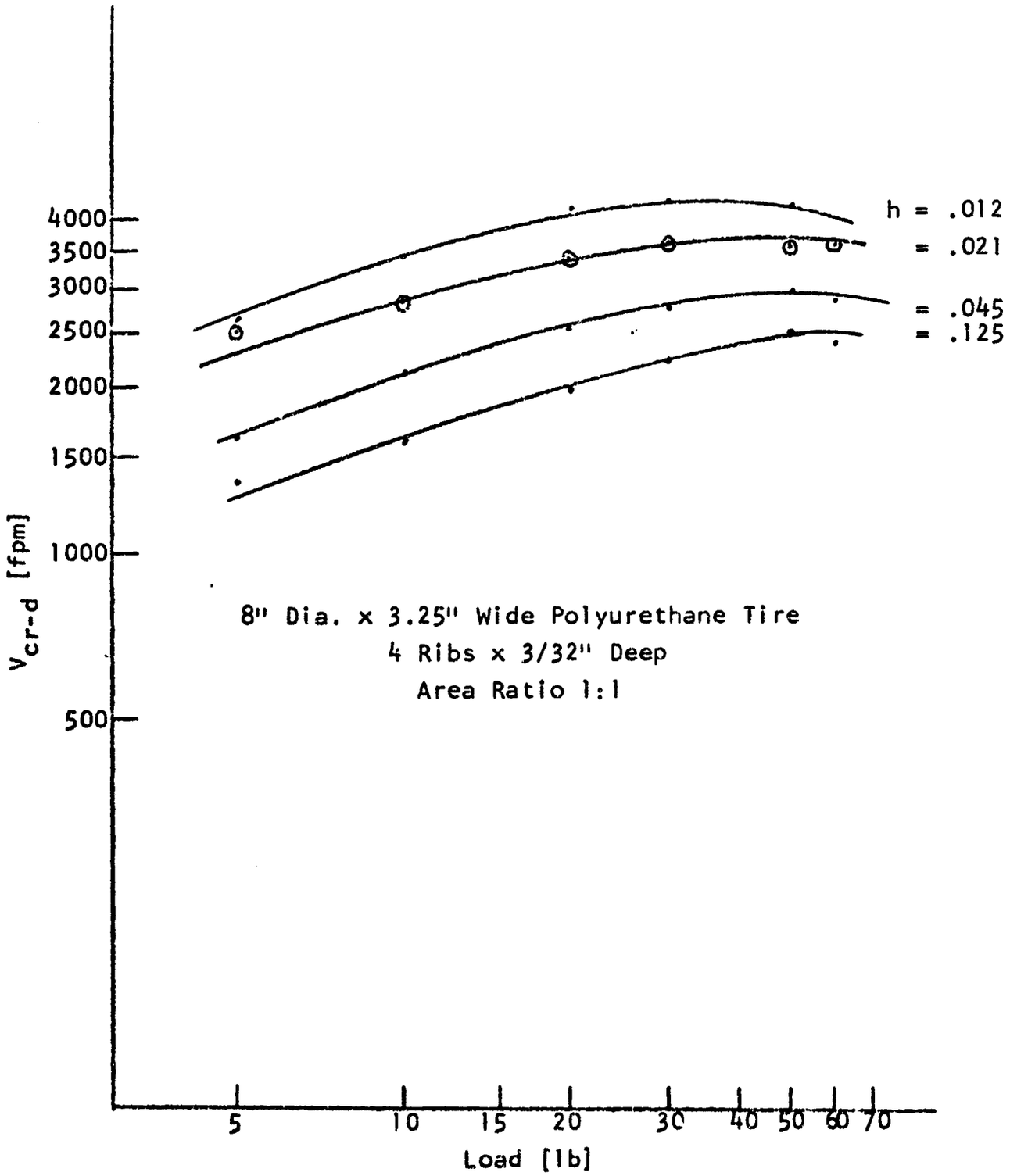

FIGURE 18. SPIN DOWN SPEED VS. LOAD (WATER FILM THICKNESS AS A PARAMETER)

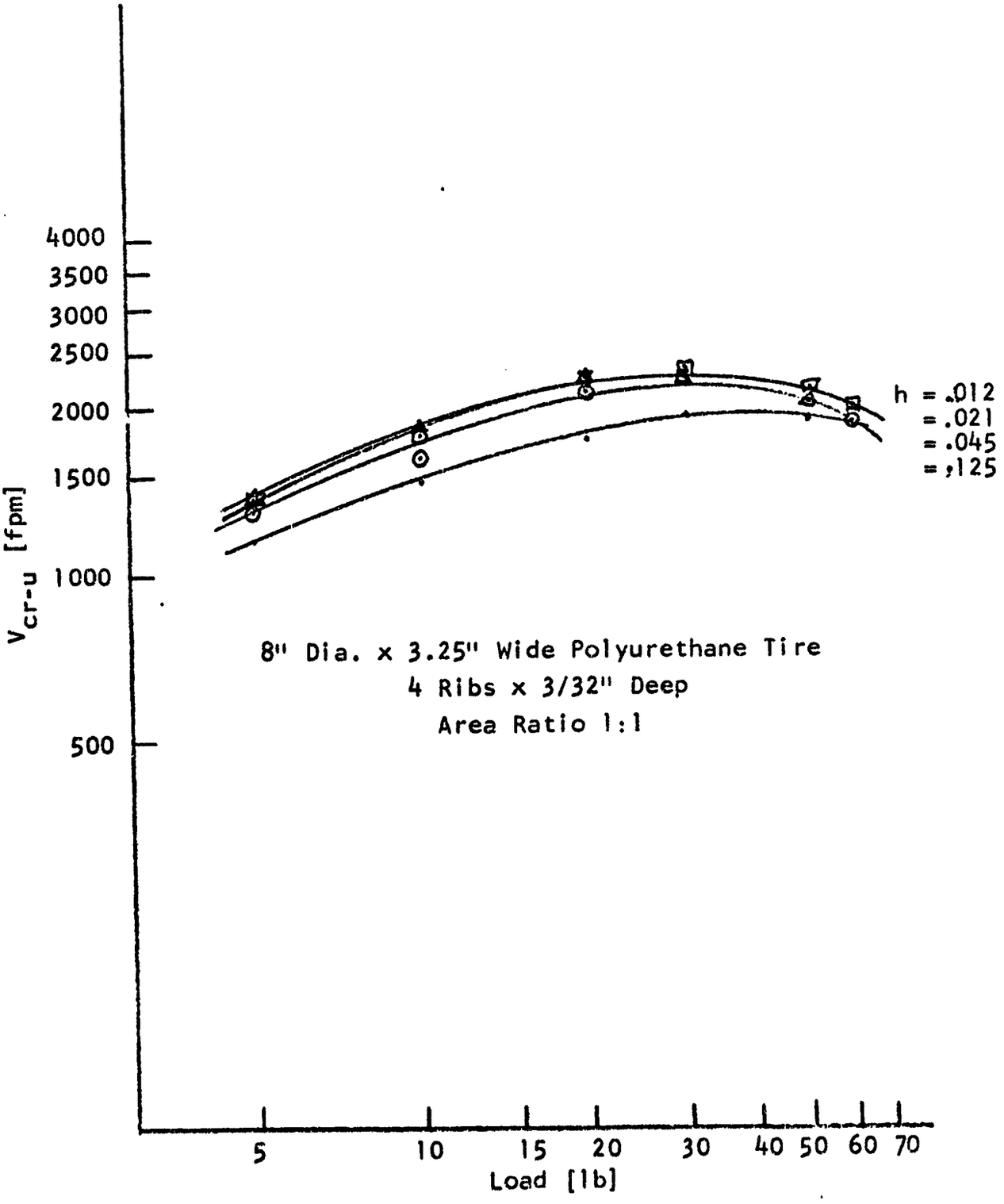

FIGURE 19. SPIN UP SPEED VS. LOAD (WATER FILM THICKNESS AS A PARAMETER)

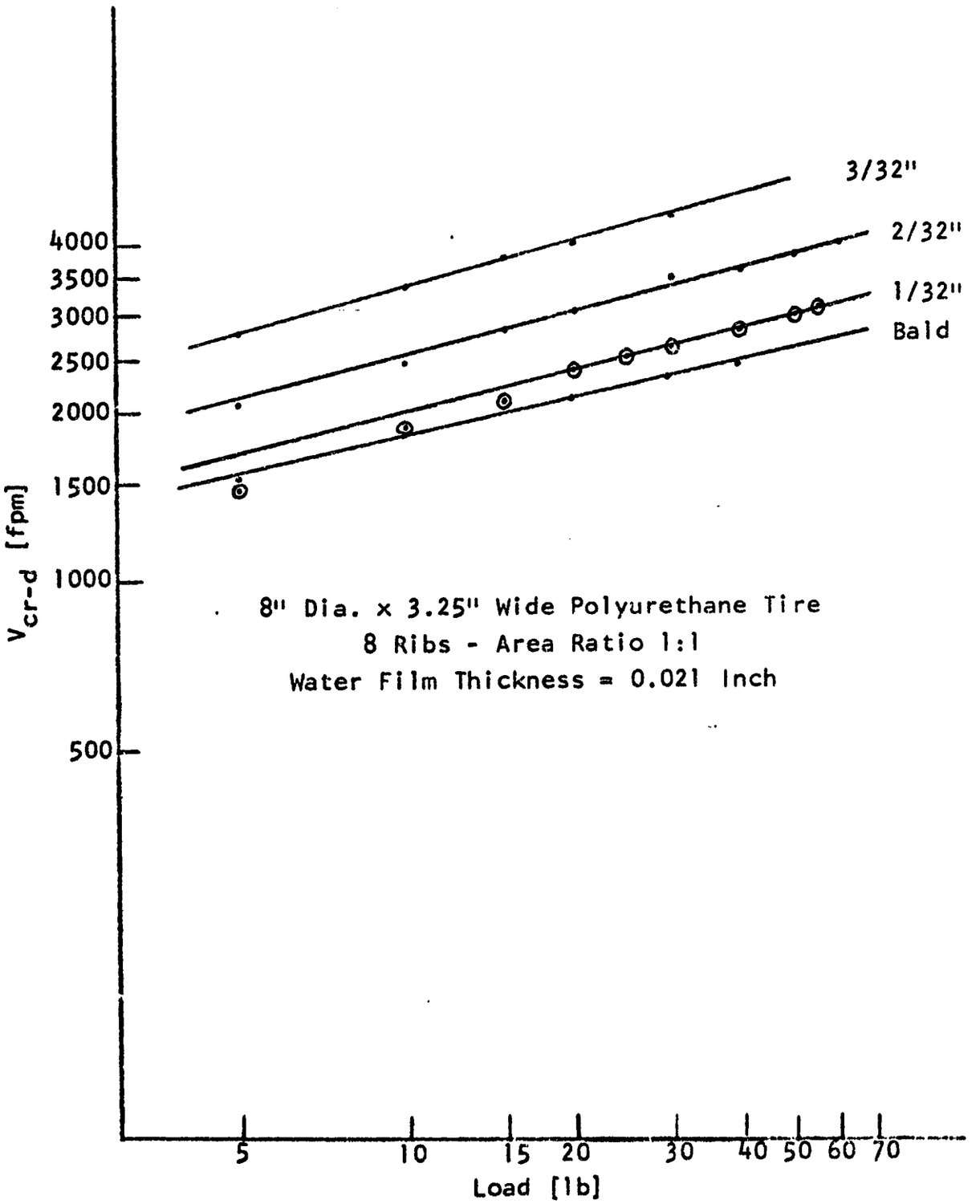

FIGURE 20. SPIN DOWN SPEED VS. LOAD (TREAD DEPTH AS A PARAMETER)

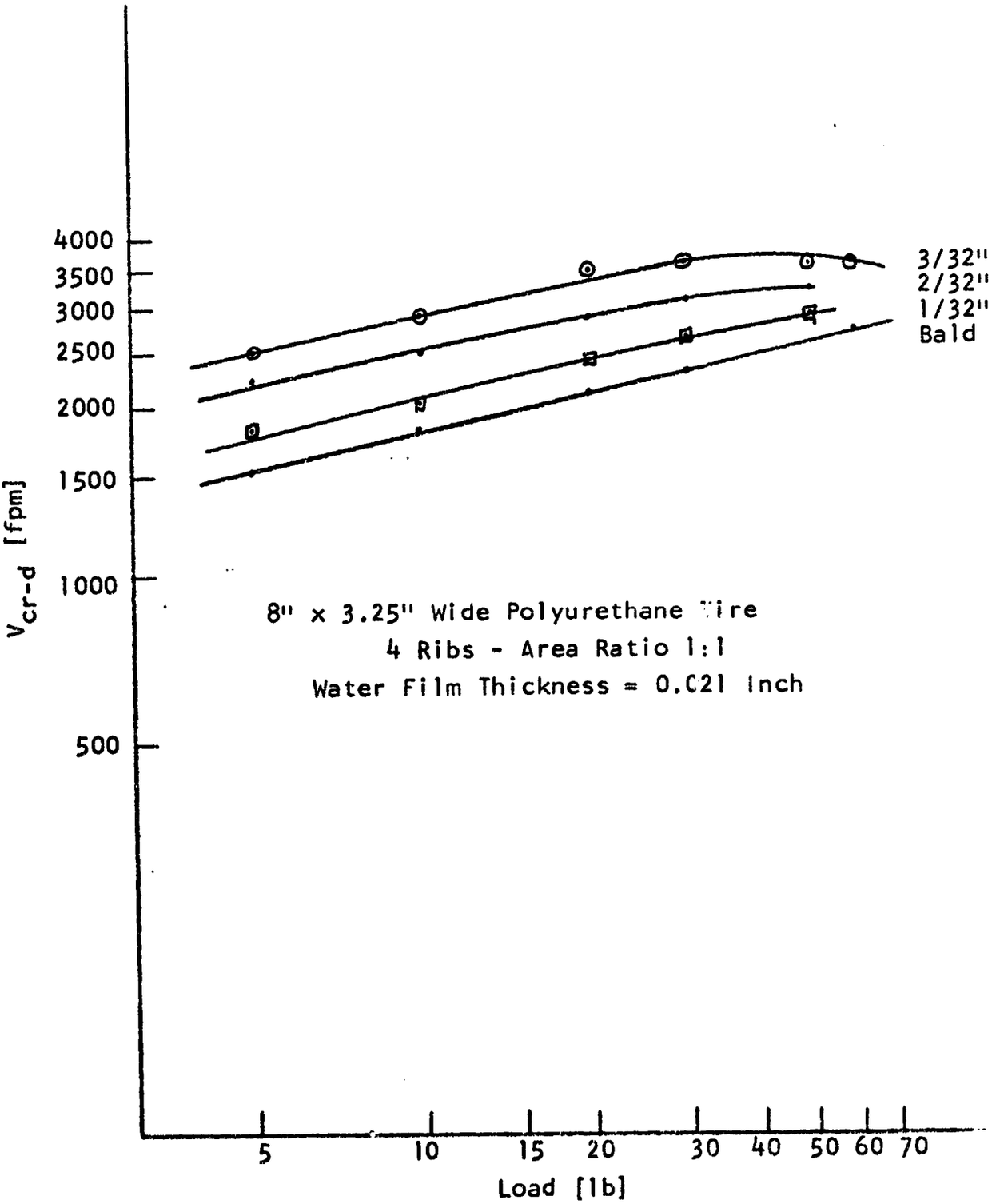

FIGURE 21. SPIN DOWN SPEED VS. LOAD (TREAD DEPTH AS A PARAMETER)

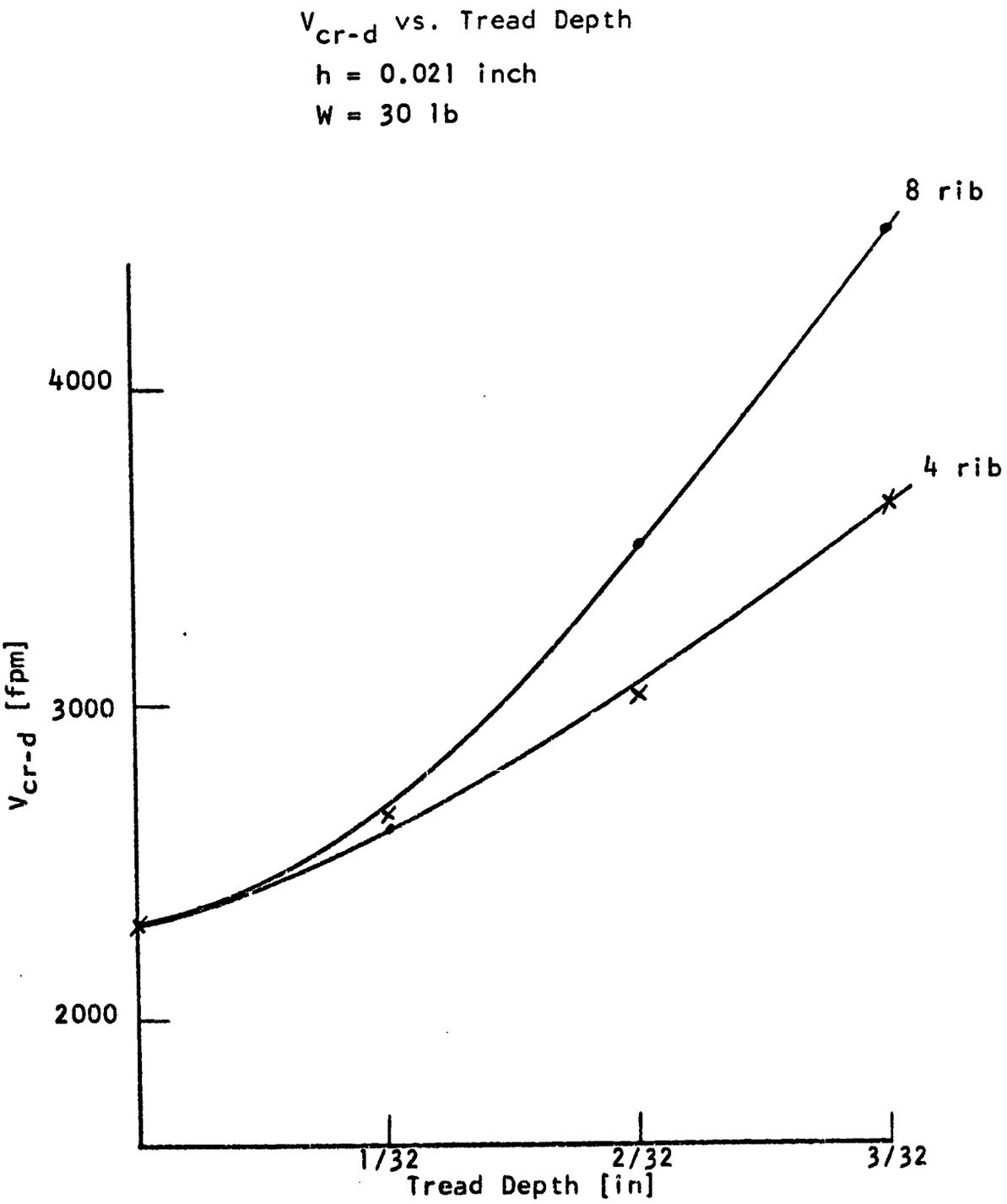

FIGURE 22. SPIN DOWN SPEED VS. TREAD DEPTH FOR A CONSTANT WATER FILM THICKNESS AND LOAD (POLYURETHANE TIRE)

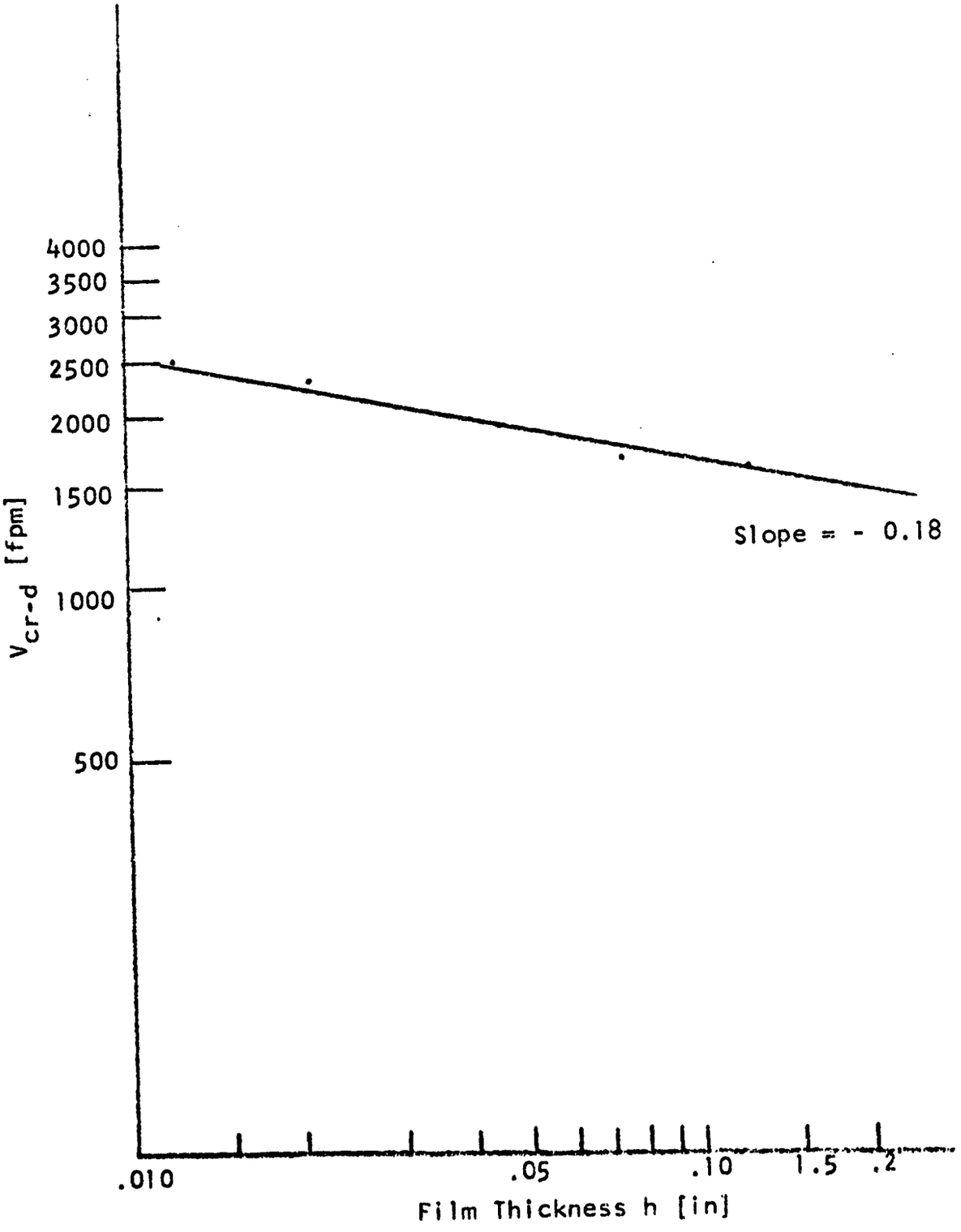

FIGURE 23. SPIN DOWN SPEED VS. WATER FILM THICKNESS
8" DIA. x 3.25" WIDE BALD POLYURETHANE
TIRE - LOAD = 30 LB

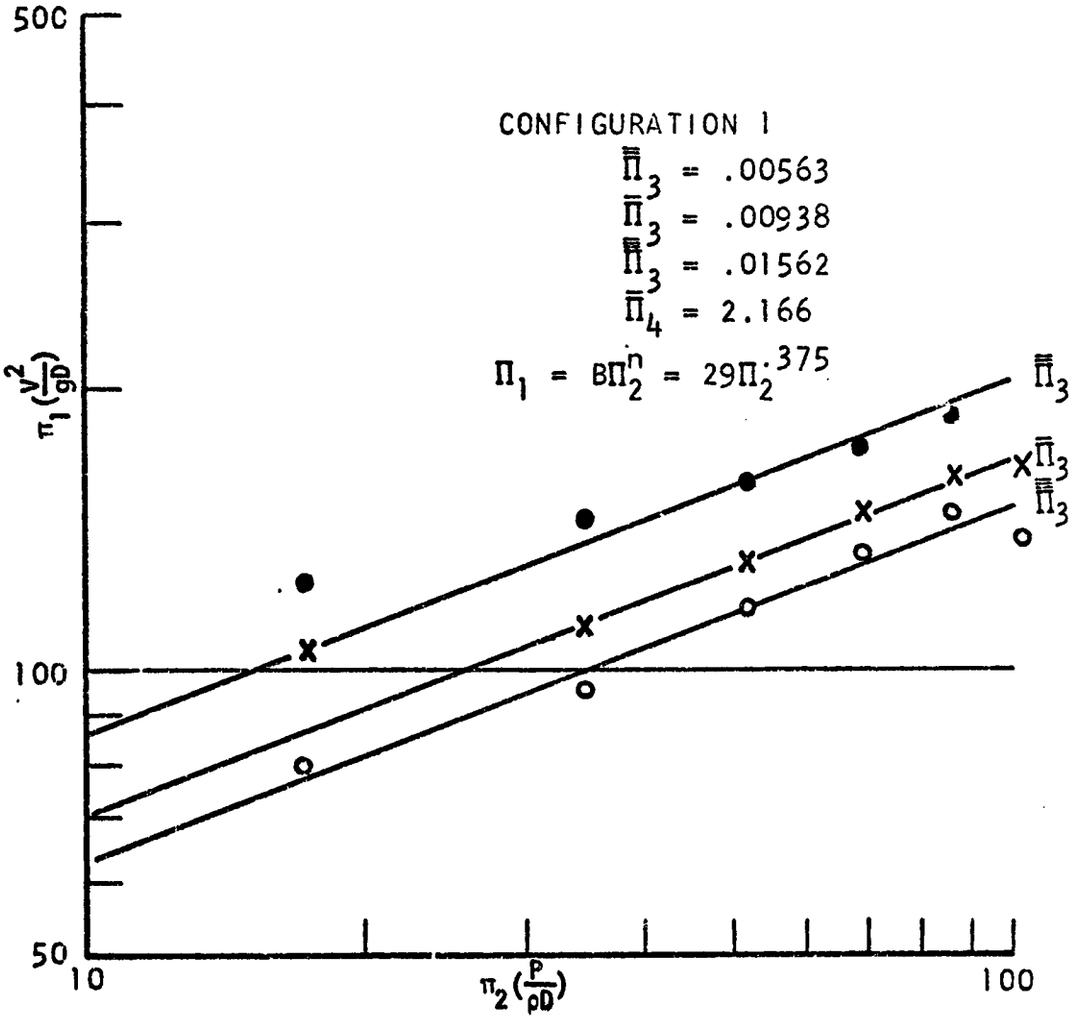

FIGURE 24. CONFIGURATION 1, Π_1 vs. Π_2

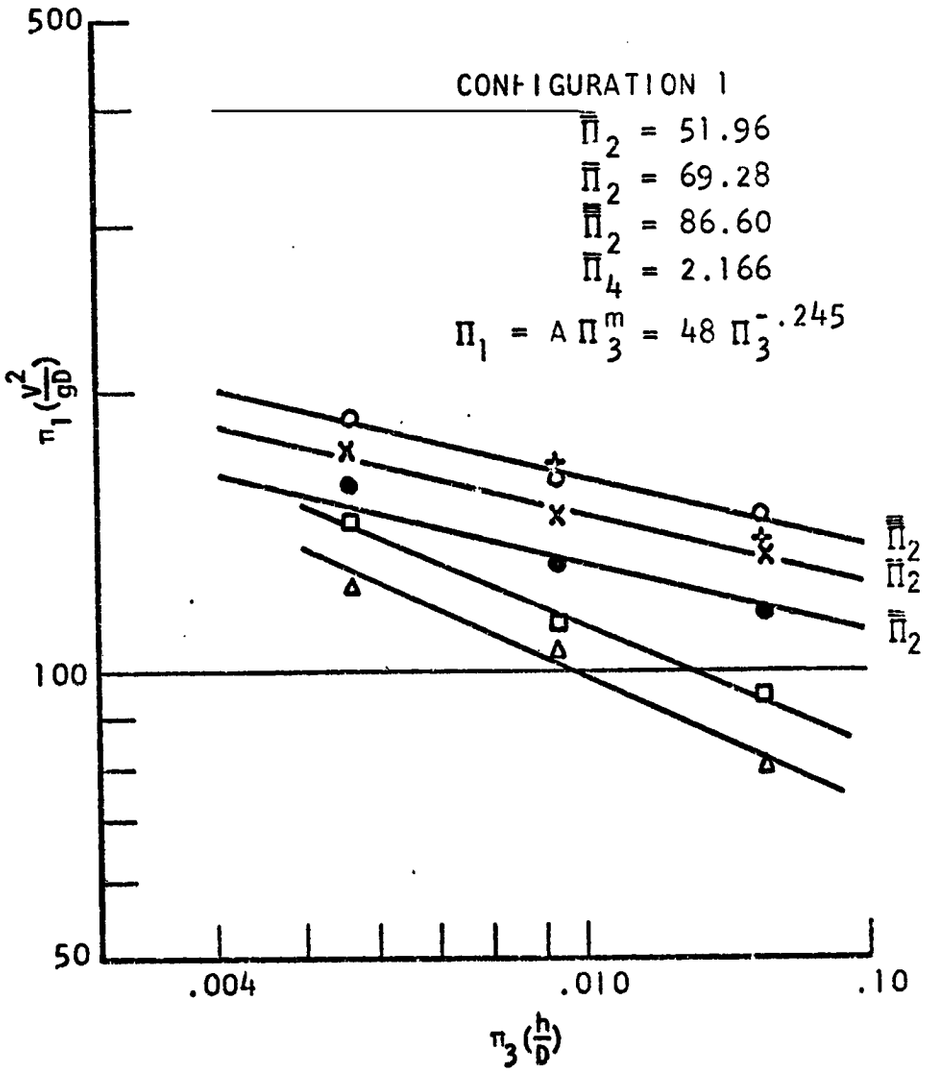

FIGURE 25. CONFIGURATION 1, Π_1 vs. Π_3

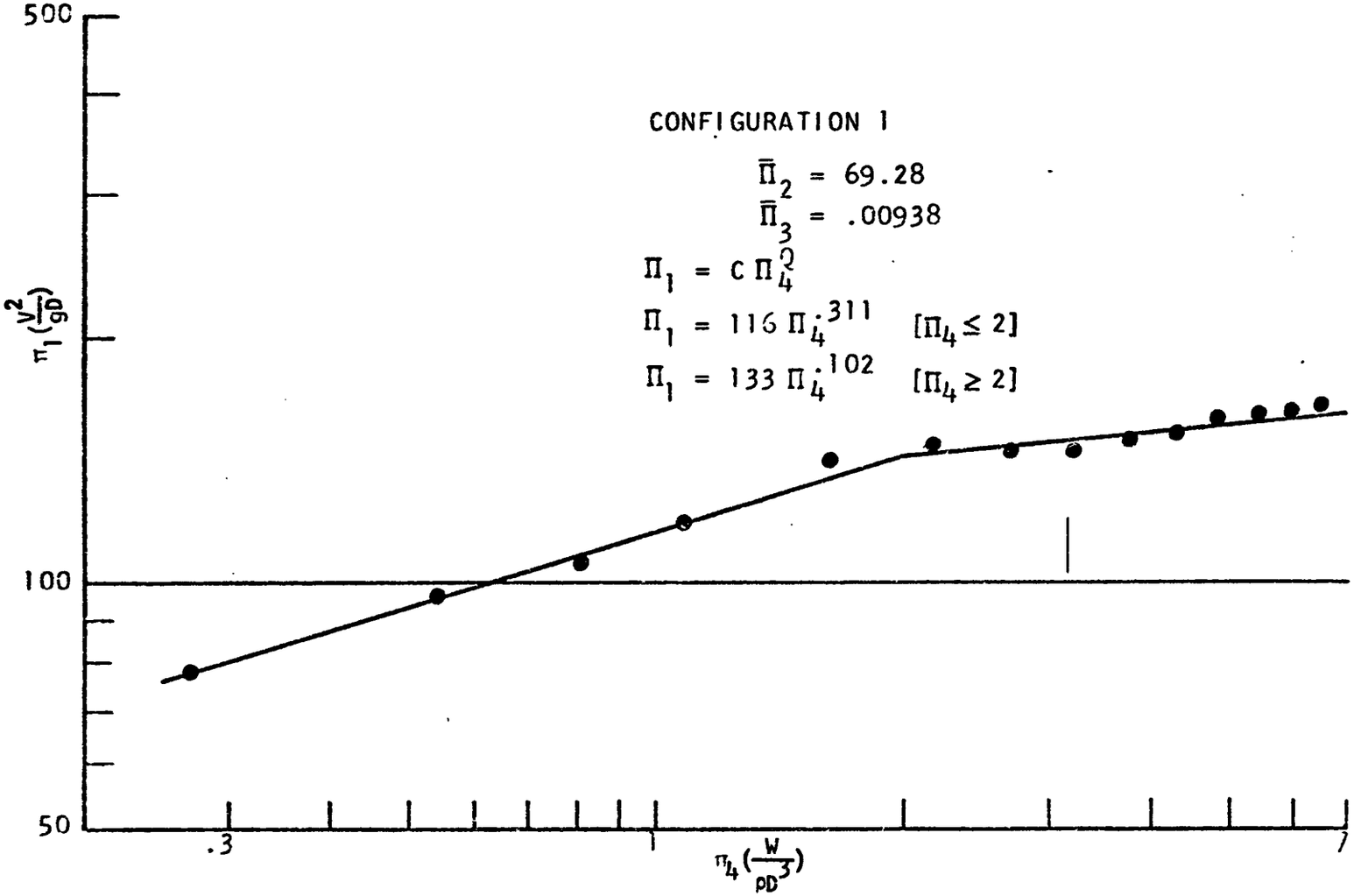

FIGURE 26. CONFIGURATION 1, Π_1 vs. Π_4

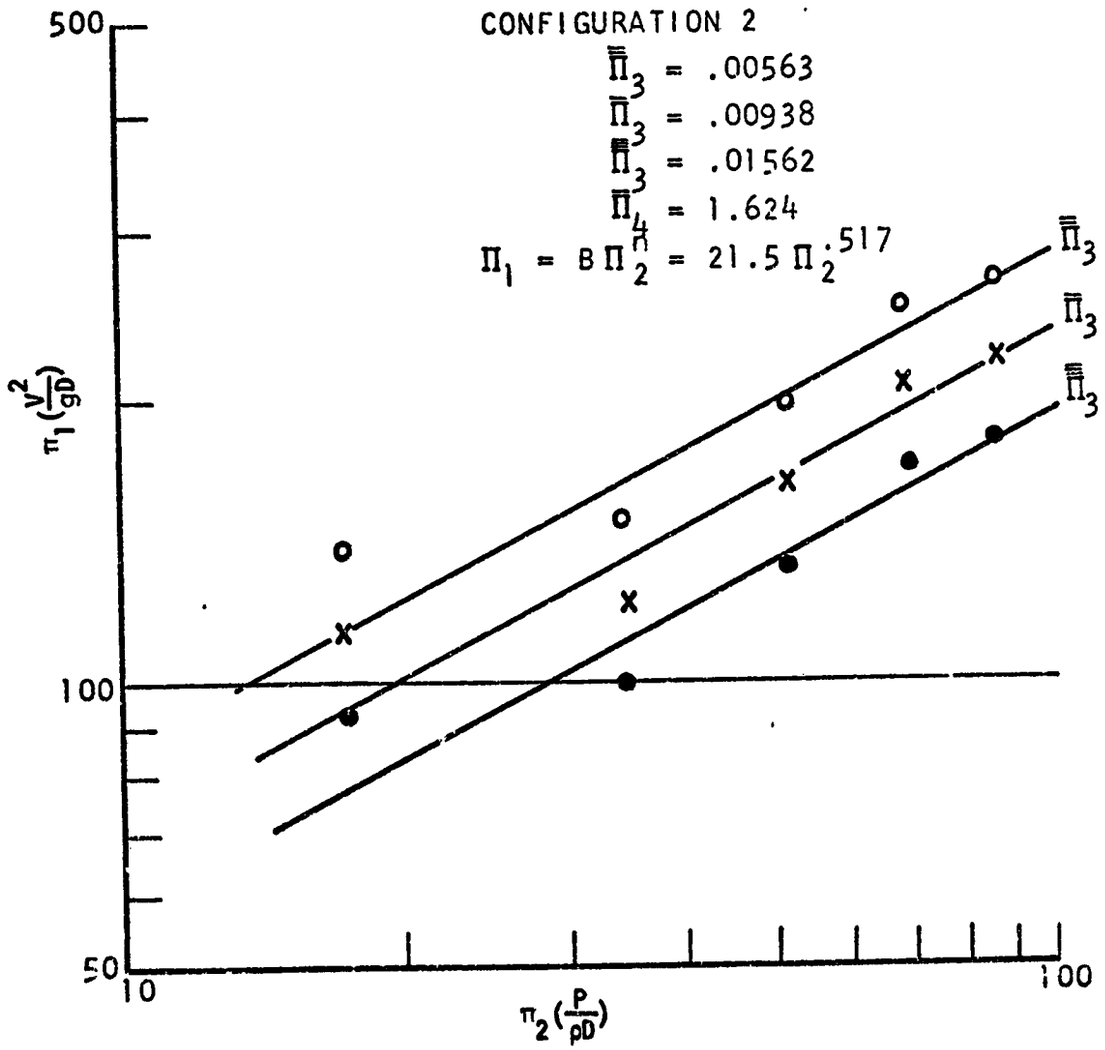

FIGURE 27. CONFIGURATION 2, Π_1 vs. Π_2

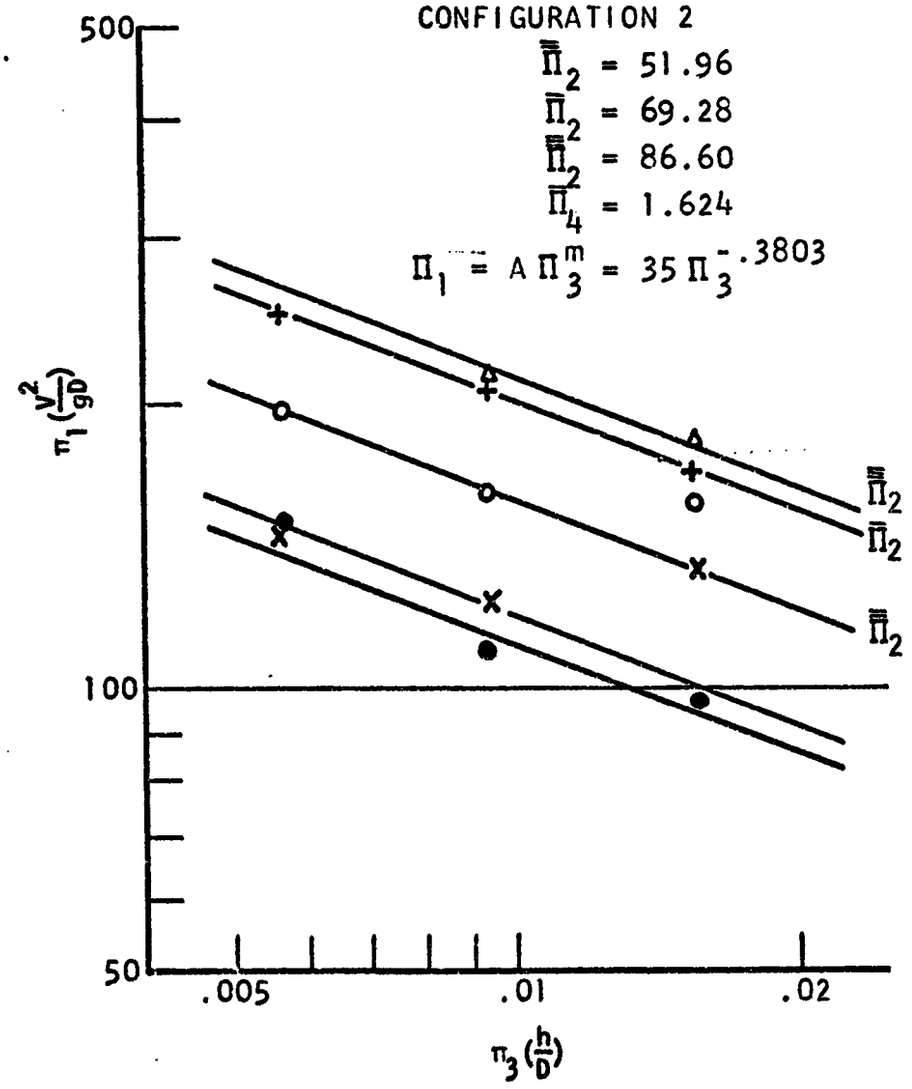

FIGURE 28. CONFIGURATION 2, Π_1 vs. Π_3

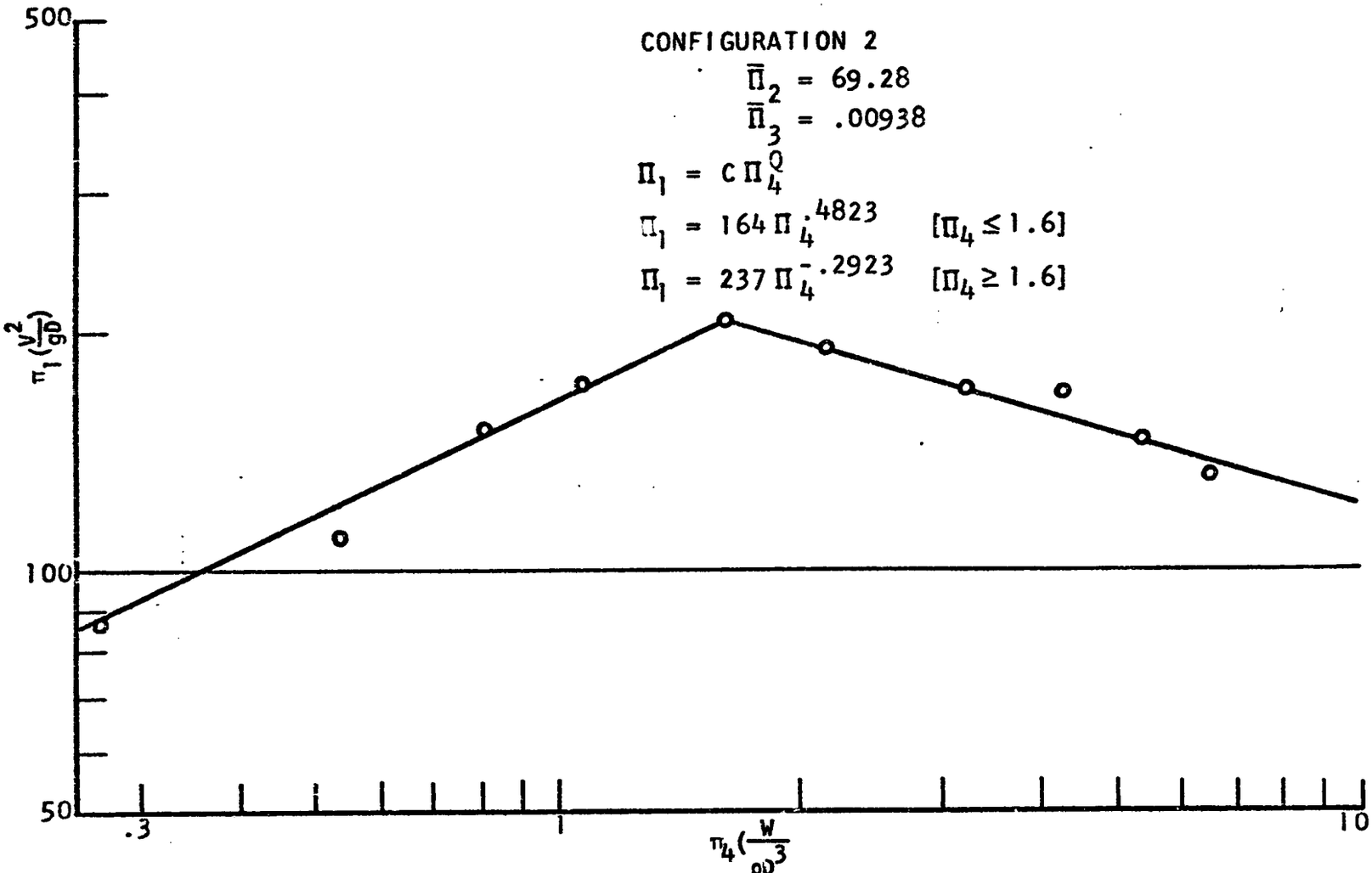

FIGURE 29. CONFIGURATION 2, Π_1 vs. Π_4

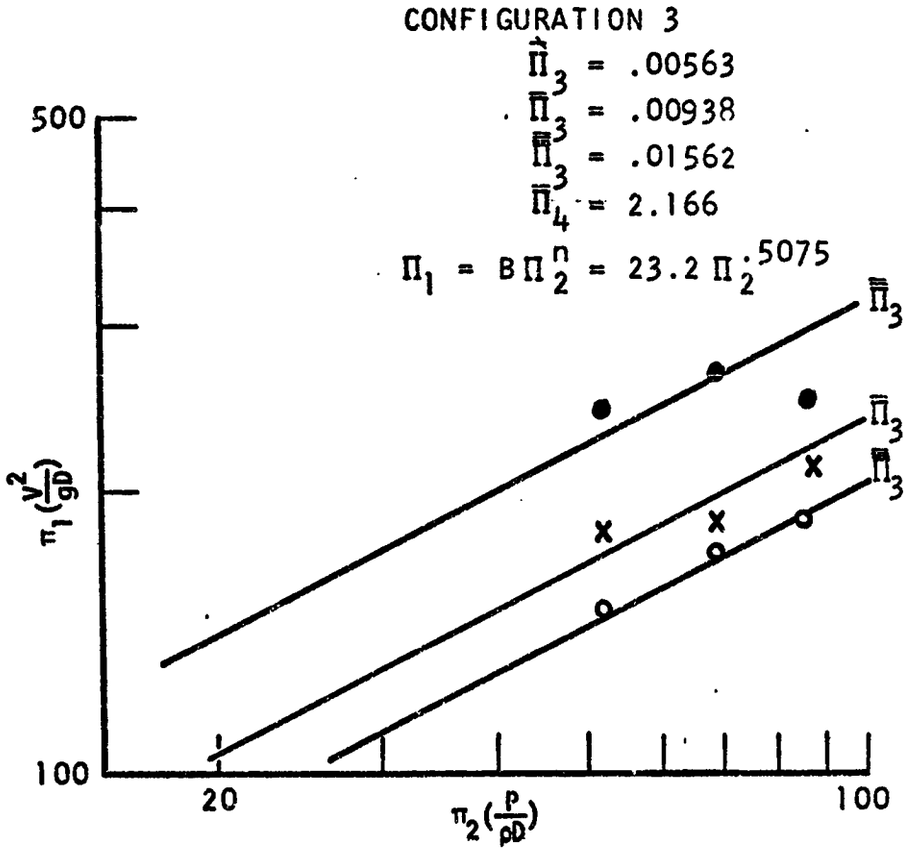

FIGURE 30. CONFIGURATION 3, Π_1 vs. Π_2

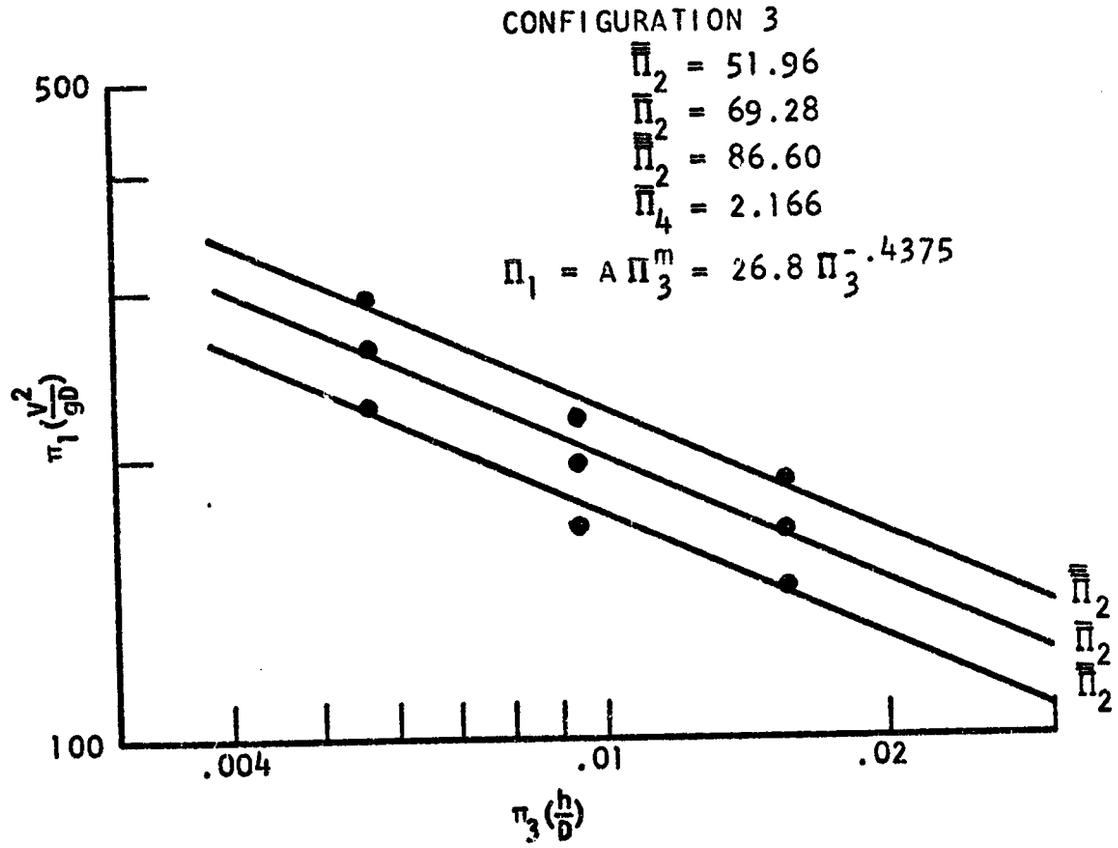

FIGURE 31. CONFIGURATION 3, Π_1 vs. Π_3

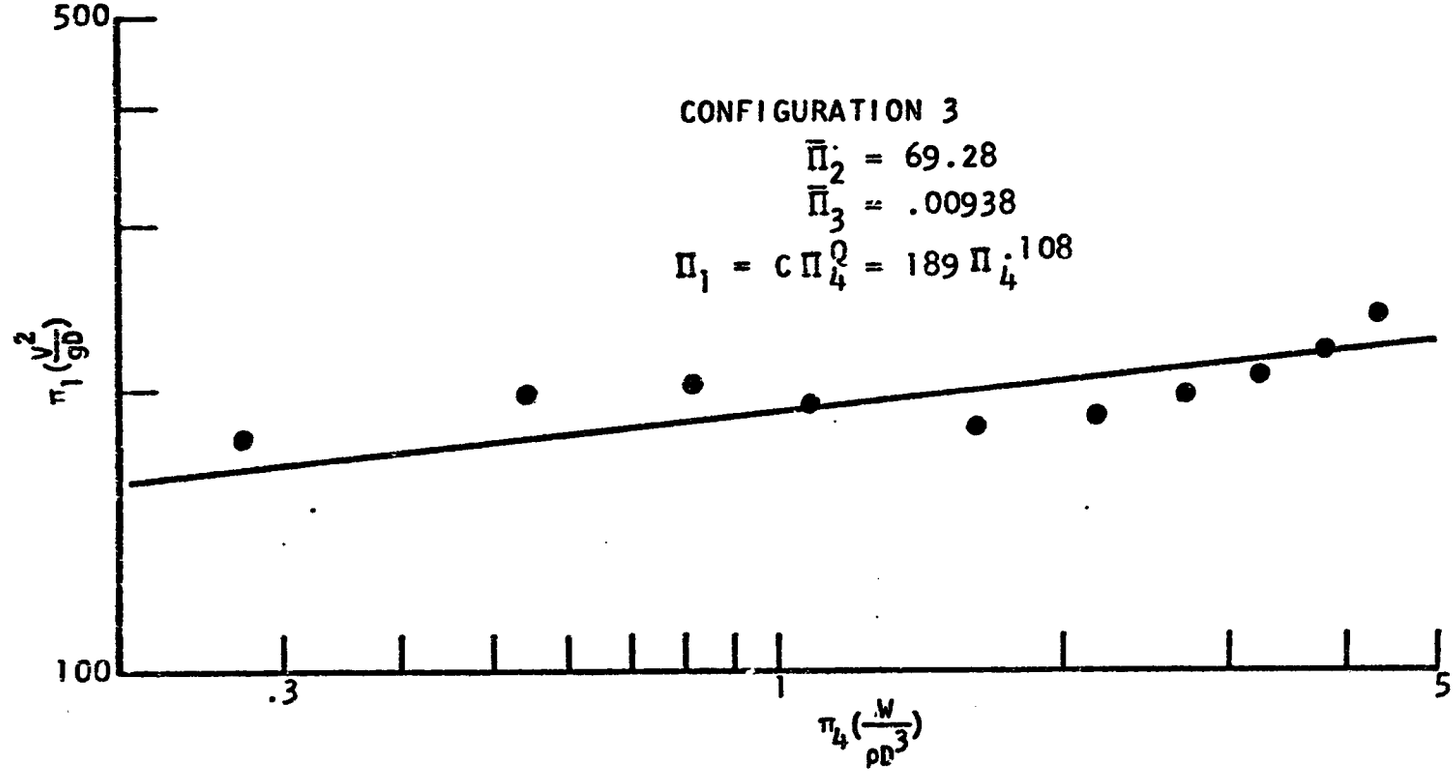

FIGURE 32. CONFIGURATION 3, Π_1 vs. Π_4

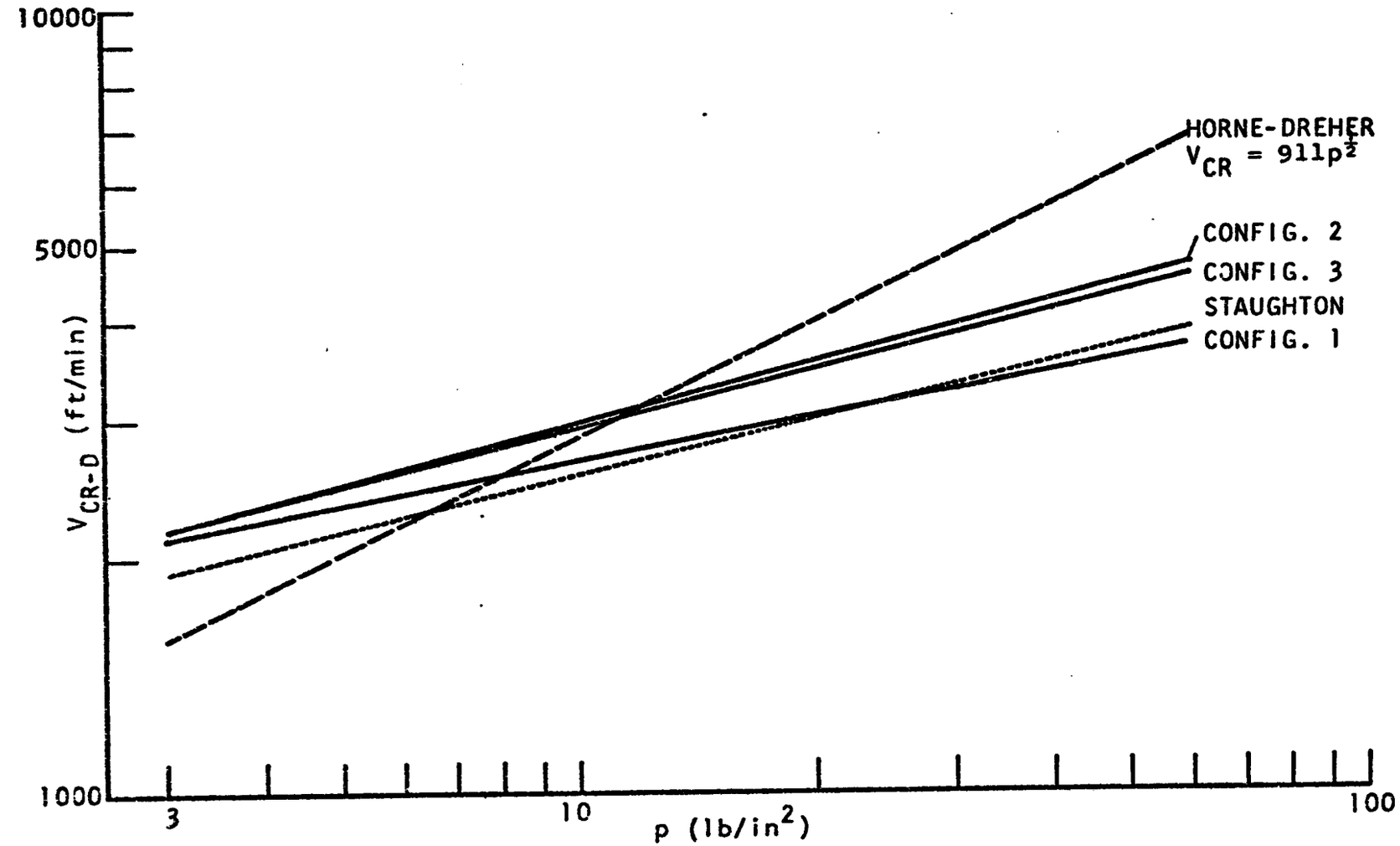

FIGURE 33. COMPARISON OF PREDICTION EQUATIONS WITH HORNE-DREHER EQUATION AND STAUGHTON EXPERIMENTAL DATA

REFERENCES

1. Dugoff, H. and Ehrlich, I. R., Proceedings of the Seventh Annual National Conference on Environmental Sciences, Princeton, New Jersey, September 1967.

2. Dugoff, H. and Ehrlich, I. R., "A Laboratory Scale Model Technique for Investigating Pneumatic Tire Hydroplaning," Davidson Laboratory Report 1223, Stevens Institute of Technology, Hoboken, New Jersey, September 1967.

3. Ehrlich, I. R., Schaefer, A. R., and Wray, G. A., "Parameters Affecting Model-Tire Hydroplaning and Rolling Restoration," Davidson Laboratory Report SIT-DL-70-1405, Stevens Institute of Technology, Hoboken, New Jersey, March 1970.

4. Wray, G. A., Jurkat, M. P., "Derivation of an Empirical Equation Relating Critical Hydroplaning Speed, Water Film Thickness and Nominal Contact Patch Bearing Pressure, for an 8" Diameter Polyurethane Model Tire," Davidson Laboratory Letter Report SIT-DL-70-1479, Stevens Institute of Technology, Hoboken, New Jersey, February 1970.

5. Horne, W. B., and Joyner, U. T., "Pneumatic Tire Hydroplaning and Some Effects on Vehicle Performance," Society of Automotive Engineers Paper 970C, January 1965.

6. Tsakonas, S., Henry, C. J., and Jacobs, W. R., "Hydrodynamics of Aircraft Tire Hydroplaning," NASA Contract Report 1125 (DL Report 1238), August 1968.

7. Daughaday, H. and Tung, C., "A Mathematical Analysis of Hydroplaning Phenomena," Cornell Aeronautical Laboratory Report AG-2495-S-1, January 1969.

8. Dugoff, H., "The Davidson Laboratory Rolling Road Facility," Davidson Laboratory Note 693, Stevens Institute of Technology, Hoboken, New Jersey, November 1963.

9. Murphy, G., "Similitude in Engineering," Ronald Press, New York, New York, 1950.

10. Staughton, G. C. and Williams, T., "Tyre Performance in Wet Surface Conditions," Road Research Laboratory, Ministry of Transport, RRL Report LR-355, Crowthorne, England, 1970.

References (cont'd)

11. Martinez, J. E., Lewis, J. M. and Stocker, A. J., "A Study of Variables Associated with Wheel Spin-Down and Hydroplaning," Texas Transportation Institute Report 147-1, March 1972.

12. Nordström, O., "Effects of the Thickness of the Water Film on Skid Resistance," paper not yet published.

BIBLIOGRAPHY

Dugoff, H. and Ehrlich, I. R., "Laboratory Scale Model Experiments to Investigate Aircraft Tire Hydroplaning," Davidson Laboratory Note 779, Hoboken, New Jersey, September 1967.

Ehrlich, I. R., "Model Studies in Tire Hydroplaning," Proceedings of the First International Conference on Vehicle Mechanics, and Davidson Laboratory Technical Note 792, Hoboken, New Jersey, undated.

Eshel, A., "A Study of Tires on a Wet Runway," AMPEX Corporation, Report RR 67-24, September 1967.

Gough, V. E. and Badger, D. W., "Tyres and Road Safety," Fifth World Meeting of the International Road Federation, Dunlop Rubber Company Ltd., London, England, 1966.

Horne, W. B. and Dreher, R. C., "Phenomena of Pneumatic Tire Hydroplaning," NASA Technical Note TN-D-2056, Washington, D. C., November 1963.

Horne, W. B. and Joyner, U. T., "Determining Causation of Aircraft Skidding Accidents or Incidents," Report presented at the 23rd Annual International Air Safety Seminar, Washington, D. C., 1970.

Horne, W. B., Joyner, U. T. and Leland, T. J. W., "Studies of the Retardation Force Developed on an Aircraft Tire Rolling in Slush or Water," NASA Technical Note D-552, Washington, D. C., September 1960.

Horne, W. B., Yager, T. J. and Taylor, G. R., "Review of Causes and Alleviation of Low Tire Traction on Wet Runways," NASA Technical Note TN-D-4406, Washington, D. C., April 1968.

I'Anson, R., "Aquaplaning Studies Using a Small Pneumatic Tire," Dept. of Aeronautical Engineering, University of Bristol, Report No. PG-70-1, Bristol, England, January 1970.

Kummer, H. W., "Pavement Wetting and Skid Resistance," Joint Road Friction Program of the Pennsylvania State Dept. of Highways, The Pennsylvania State University, Report No. 8, University Park, Pennsylvania, December 1963.

Ludema, K. C., "Road Surface Texture," Materials Research and Standards, October 1971.

Moore, D. F., "A Study of Tire-Surface Interaction for the Case of Rolling on a Wet Surface," Cornell Aeronautical Laboratory, Report No. YD-1969-V-2, Buffalo, New York, July 1965.

Moore, D. F., "Drainage Criteria for Runway Surface Roughness," Cornell Aeronautical Laboratory, Report No. 139, Buffalo, New York, December 1963.

Nordström, O., "The Effect of the Depth of Water Films on Road Friction," from a draft of Chapter III from the P.I.A.R.C. Technical Committee on Slipperiness, Statens Väginstitut, Stockholm, Sweden, December 1970.

Rose, J. G., "Pavement Surface Texture Measurement Methods," an Interim Report prepared by ASTM Subcommittee E-17.23, Atlantic City, New Jersey, June 1971.